

Figure 1. Average Binder cumulant of magnetization (left) and polarization (right) for the 2-color Ashkin-Teller model with $\epsilon = 1/4$. The data have been obtained using Algo. 1 with 4 states per site.

Improved Matrix Product Operator Renormalization Group: application to the 3-color random Ashkin-Teller chain

Christophe Chatelain

Université de Lorraine, CNRS, LPCT, F-54000 Nancy, France

E-mail: christophe.chatelain@univ-lorraine.fr

Abstract. Supplementary material.

PACS numbers:

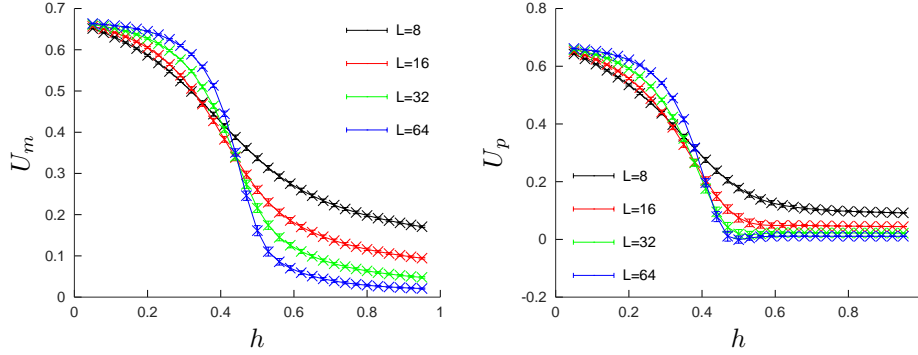


Figure 2. Average Binder cumulant of magnetization (left) and polarization (right) for the 2-color Ashkin-Teller model with $\epsilon = \sqrt{2}/4$. The data have been obtained using Algo. 1 with 4 states per site.

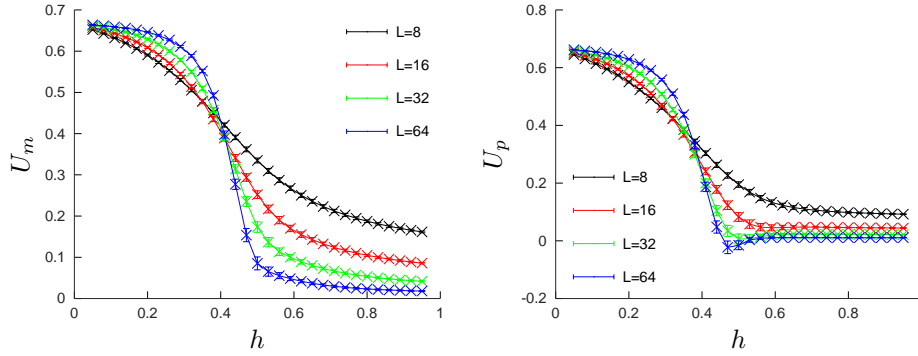


Figure 3. Average Binder cumulant of magnetization (left) and polarization (right) for the 2-color Ashkin-Teller model with $\epsilon = 1/2$. The data have been obtained using Algo. 1 with 4 states per site.

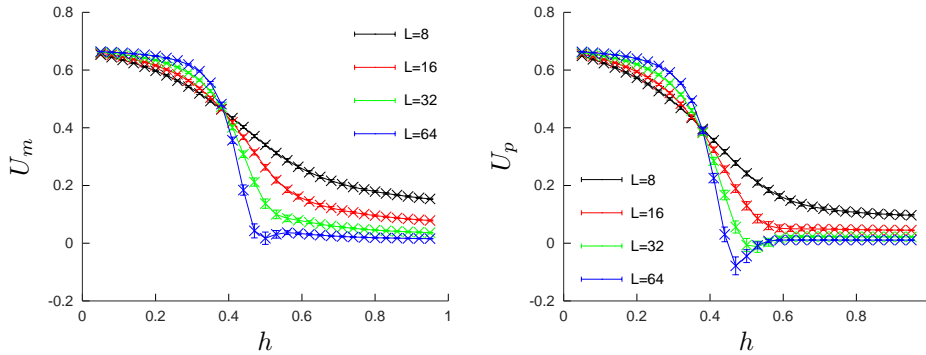


Figure 4. Average Binder cumulant of magnetization (left) and polarization (right) for the 2-color Ashkin-Teller model with $\epsilon = \sqrt{2}/2$. The data have been obtained using Algo. 1 with 4 states per site.

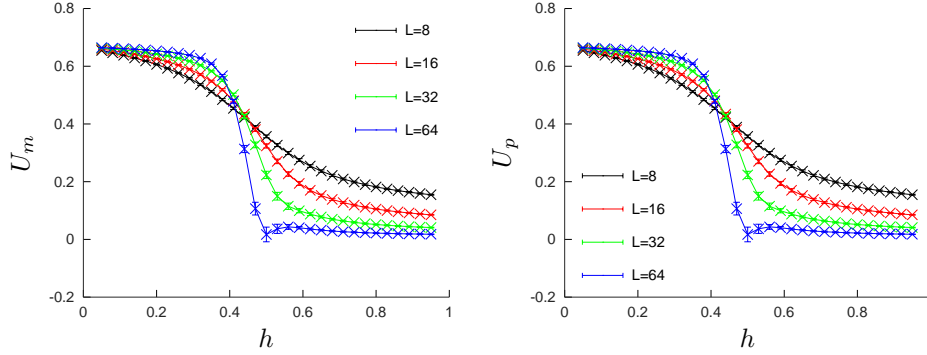


Figure 5. Average Binder cumulant of magnetization (left) and polarization (right) for the 2-color Ashkin-Teller model with $\epsilon = 1$. The data have been obtained using Algo. 1 with 4 states per site.

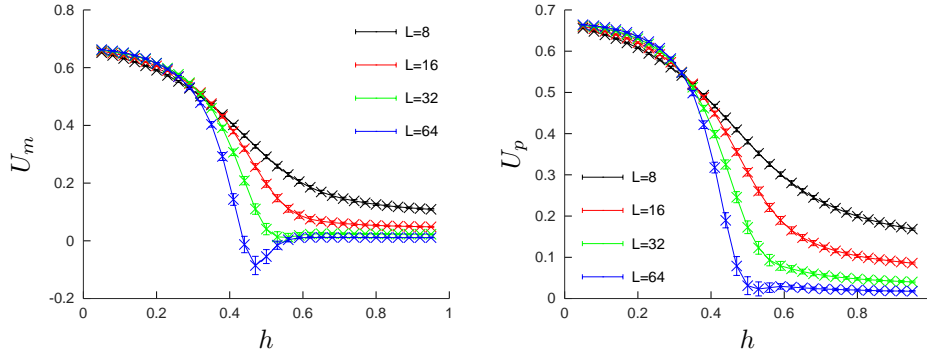


Figure 6. Average Binder cumulant of magnetization (left) and polarization (right) for the 2-color Ashkin-Teller model with $\epsilon = \sqrt{2}$. The data have been obtained using Algo. 1 with 4 states per site.

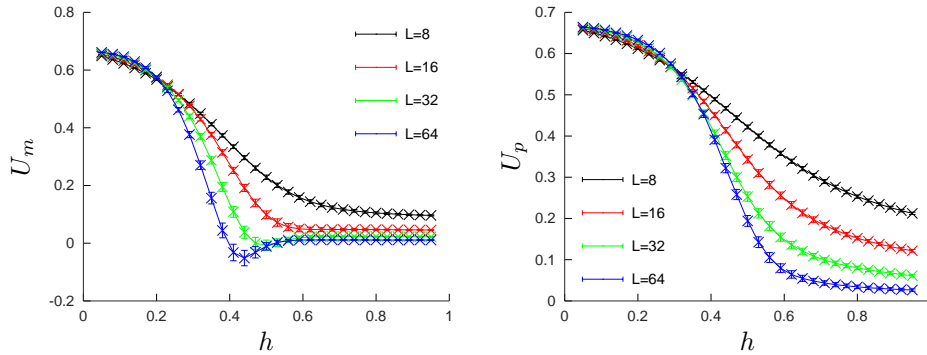


Figure 7. Average Binder cumulant of magnetization (left) and polarization (right) for the 2-color Ashkin-Teller model with $\epsilon = 2$. The data have been obtained using Algo. 1 with 4 states per site.

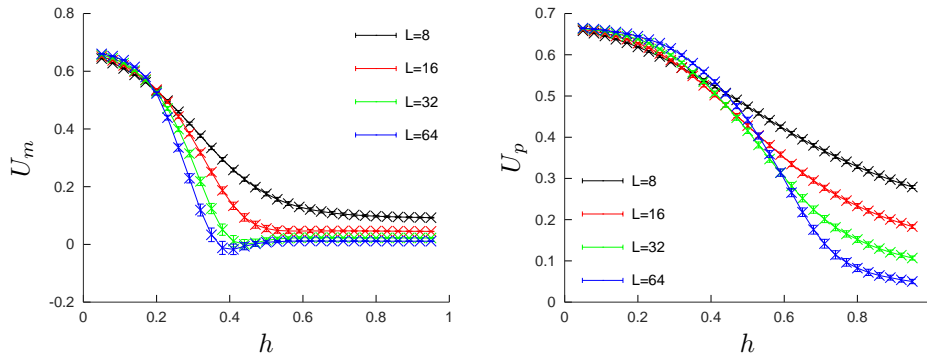


Figure 8. Average Binder cumulant of magnetization (left) and polarization (right) for the 2-color Ashkin-Teller model with $\epsilon = 2\sqrt{2}$. The data have been obtained using Algo. 1 with 4 states per site.

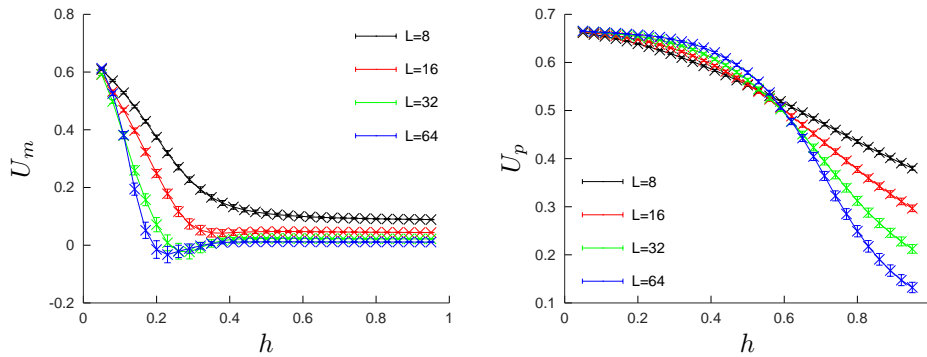


Figure 9. Average Binder cumulant of magnetization (left) and polarization (right) for the 2-color Ashkin-Teller model with $\epsilon = 4$. The data have been obtained using Algo. 1 with 4 states per site.

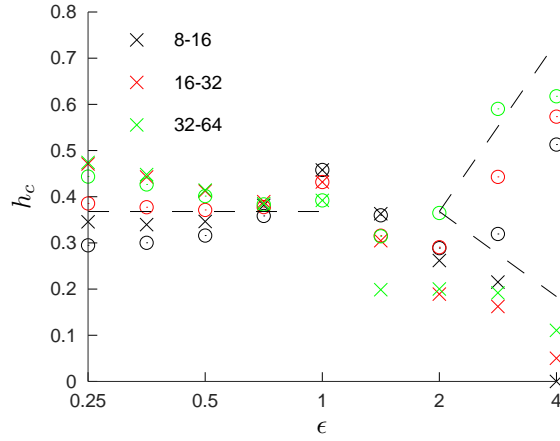


Figure 10. Phase diagram of the 2-color Ashkin-Teller model obtained from the crossings of the Binder cumulants U_m (crosses) and U_p (circles). The colors are associated to the pair of lattice sizes (see the legend) used to find the crossing of the cumulants. The data have been obtained using Algo. 1 with 4 states per site.

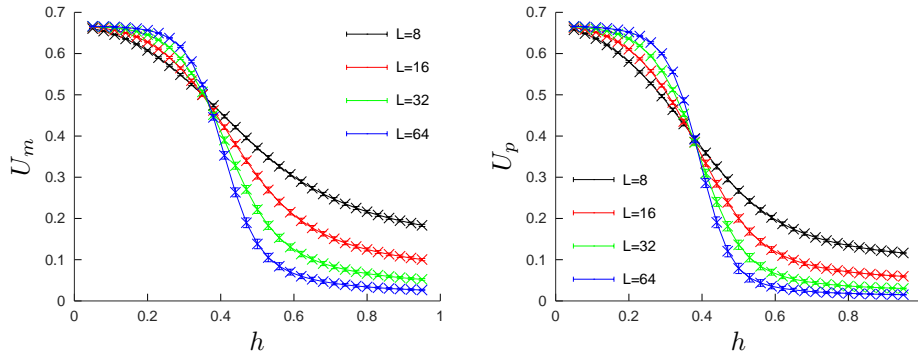


Figure 11. Average Binder cumulant of magnetization (left) and polarization (right) for the 2-color Ashkin-Teller model with $\epsilon = 1/4$. The data have been obtained using Algo. 2 with 4 states per site.

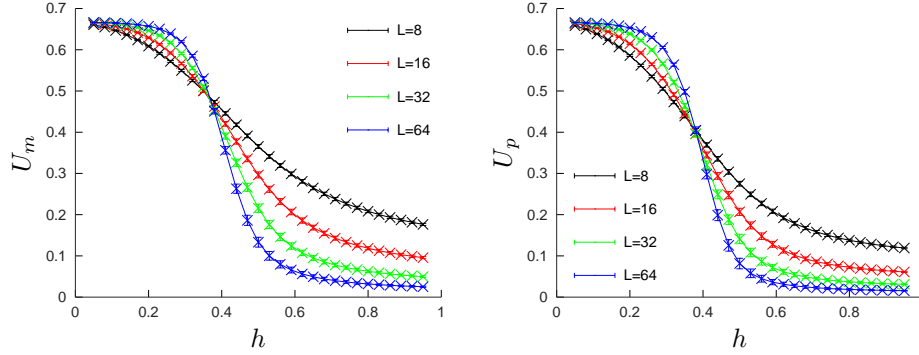


Figure 12. Average Binder cumulant of magnetization (left) and polarization (right) for the 2-color Ashkin-Teller model with $\epsilon = \sqrt{2}/4$. The data have been obtained using Algo. 2 with 4 states per site.

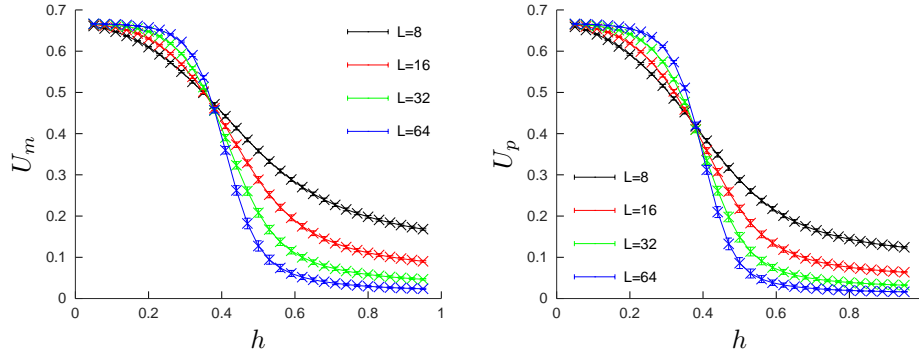


Figure 13. Average Binder cumulant of magnetization (left) and polarization (right) for the 2-color Ashkin-Teller model with $\epsilon = 1/2$. The data have been obtained using Algo. 2 with 4 states per site.

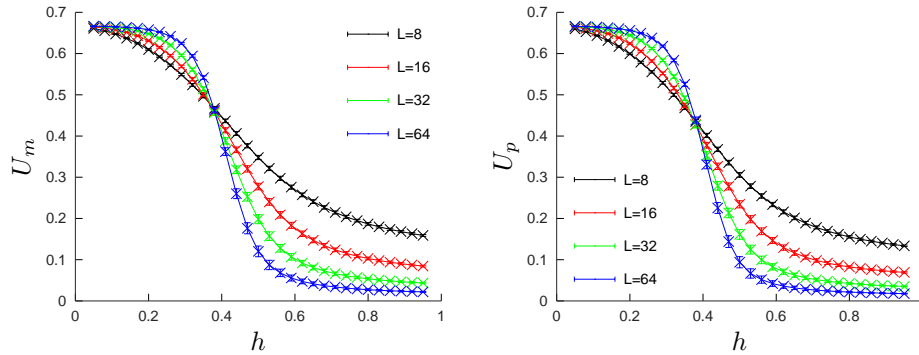


Figure 14. Average Binder cumulant of magnetization (left) and polarization (right) for the 2-color Ashkin-Teller model with $\epsilon = \sqrt{2}/2$. The data have been obtained using Algo. 2 with 4 states per site.

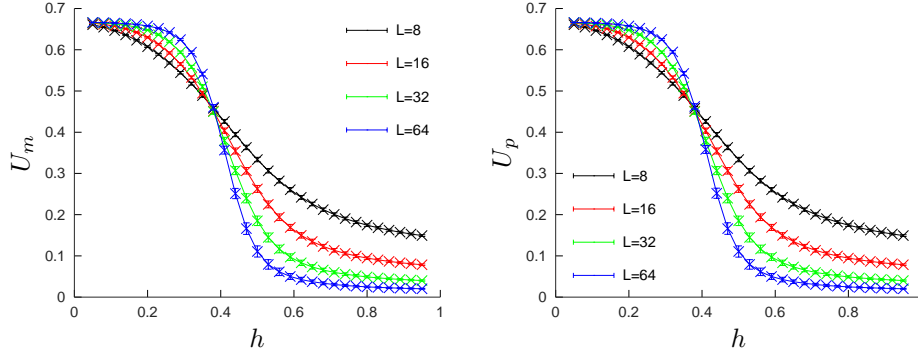


Figure 15. Average Binder cumulant of magnetization (left) and polarization (right) for the 2-color Ashkin-Teller model with $\epsilon = 1$. The data have been obtained using Algo. 2 with 4 states per site.

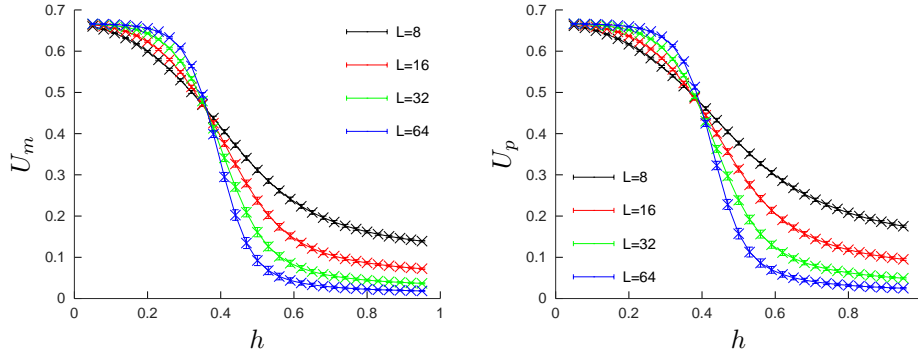


Figure 16. Average Binder cumulant of magnetization (left) and polarization (right) for the 2-color Ashkin-Teller model with $\epsilon = \sqrt{2}$. The data have been obtained using Algo. 2 with 4 states per site.

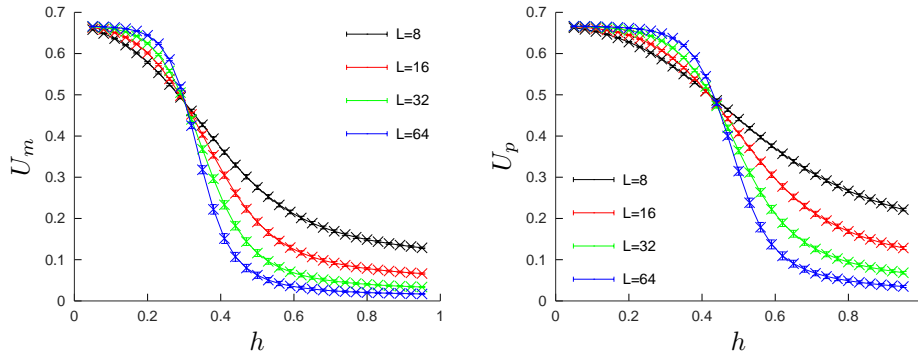


Figure 17. Average Binder cumulant of magnetization (left) and polarization (right) for the 2-color Ashkin-Teller model with $\epsilon = 2$. The data have been obtained using Algo. 2 with 4 states per site.

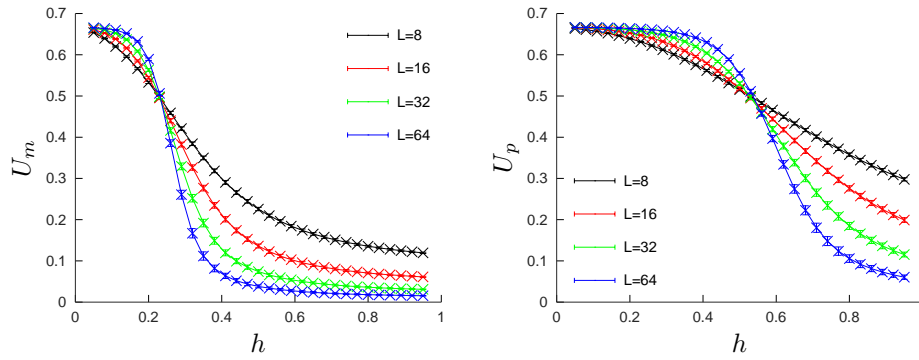


Figure 18. Average Binder cumulant of magnetization (left) and polarization (right) for the 2-color Ashkin-Teller model with $\epsilon = 2\sqrt{2}$. The data have been obtained using Algo. 2 with 4 states per site.

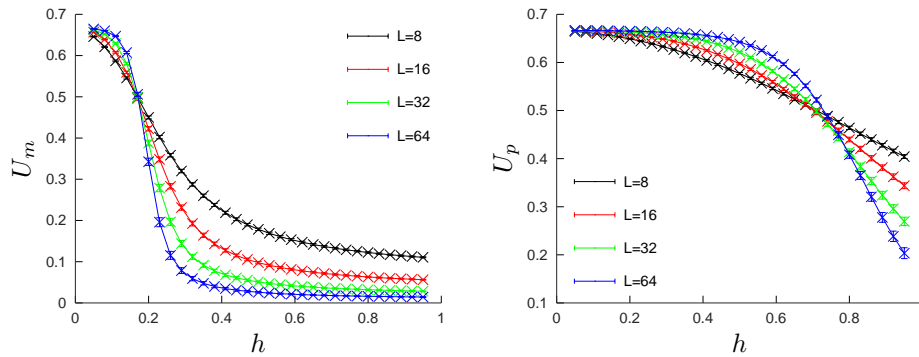


Figure 19. Average Binder cumulant of magnetization (left) and polarization (right) for the 2-color Ashkin-Teller model with $\epsilon = 4$. The data have been obtained using Algo. 2 with 4 states per site.

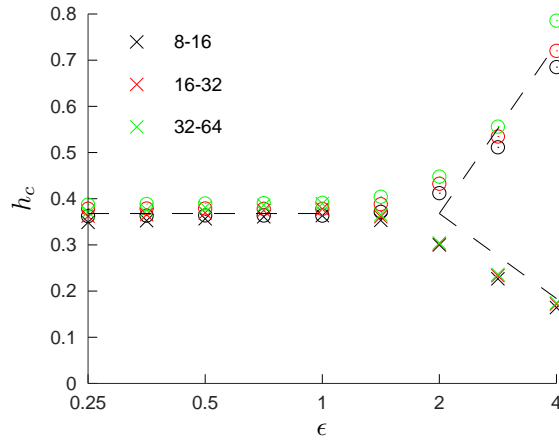


Figure 20. Phase diagram of the 2-color Ashkin-Teller model obtained from the crossings of the Binder cumulants U_m (crosses) and U_p (circles). The colors are associated to the pair of lattice sizes (see the legend) used to find the crossing of the cumulants. The data have been obtained using Algo. 2 with 4 states per site.

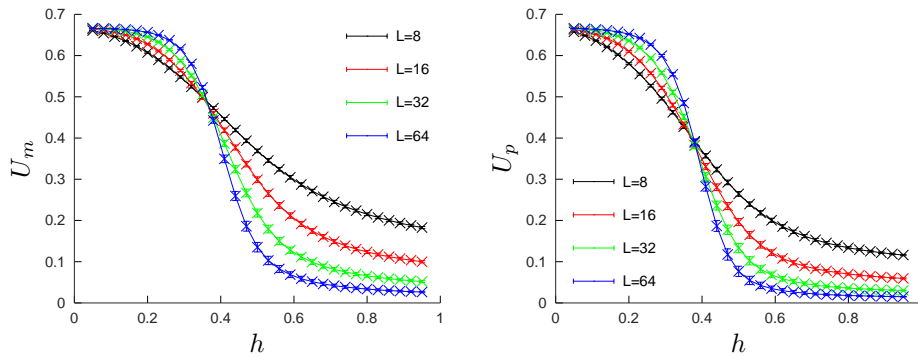


Figure 21. Average Binder cumulant of magnetization (left) and polarization (right) for the 2-color Ashkin-Teller model with $\epsilon = 1/4$. The data have been obtained using Algo. 3 with 4 states per site.

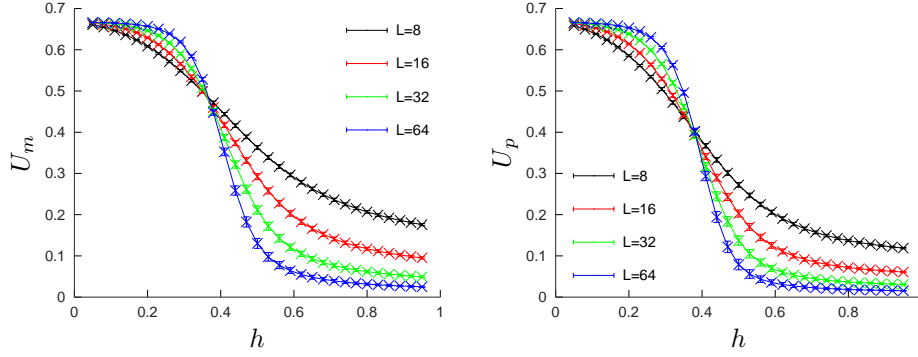


Figure 22. Average Binder cumulant of magnetization (left) and polarization (right) for the 2-color Ashkin-Teller model with $\epsilon = \sqrt{2}/4$. The data have been obtained using Algo. 3 with 4 states per site.

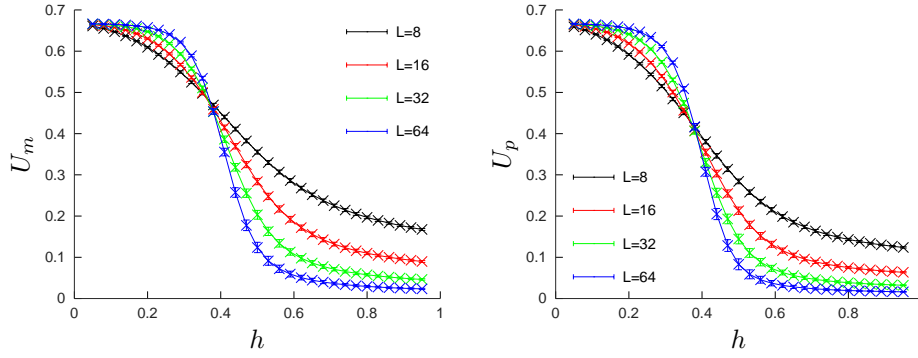


Figure 23. Average Binder cumulant of magnetization (left) and polarization (right) for the 2-color Ashkin-Teller model with $\epsilon = 1/2$. The data have been obtained using Algo. 3 with 4 states per site.

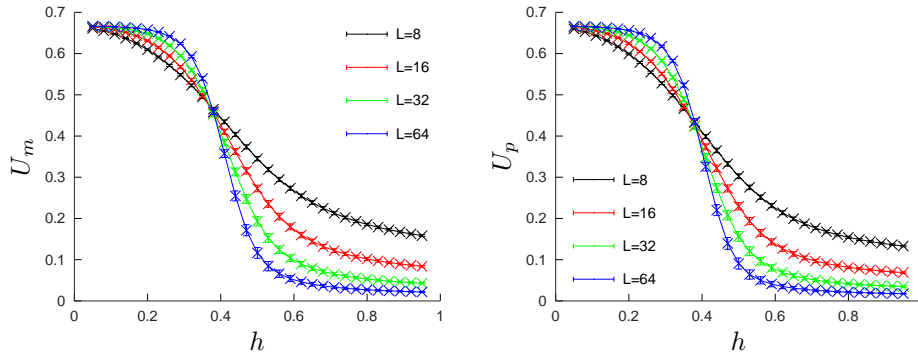


Figure 24. Average Binder cumulant of magnetization (left) and polarization (right) for the 2-color Ashkin-Teller model with $\epsilon = \sqrt{2}/2$. The data have been obtained using Algo. 3 with 4 states per site.

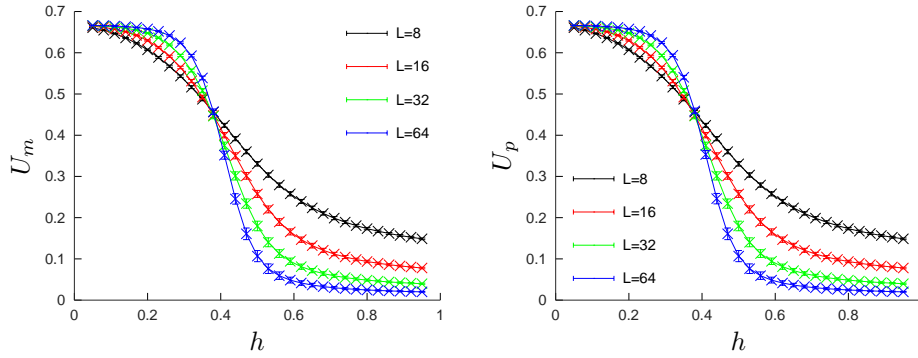


Figure 25. Average Binder cumulant of magnetization (left) and polarization (right) for the 2-color Ashkin-Teller model with $\epsilon = 1$. The data have been obtained using Algo. 3 with 4 states per site.

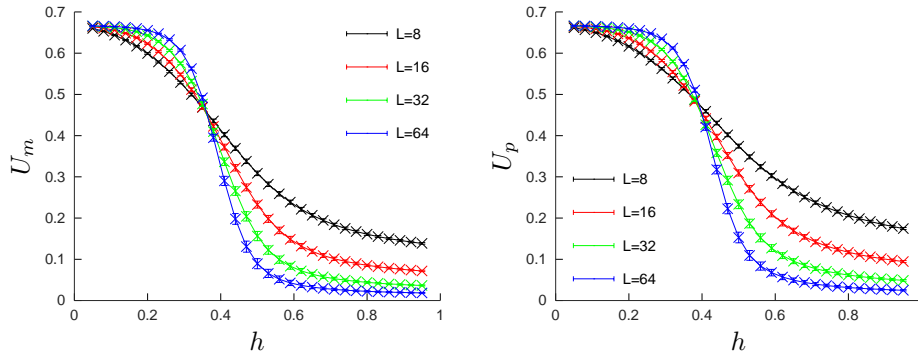


Figure 26. Average Binder cumulant of magnetization (left) and polarization (right) for the 2-color Ashkin-Teller model with $\epsilon = \sqrt{2}$. The data have been obtained using Algo. 3 with 4 states per site.

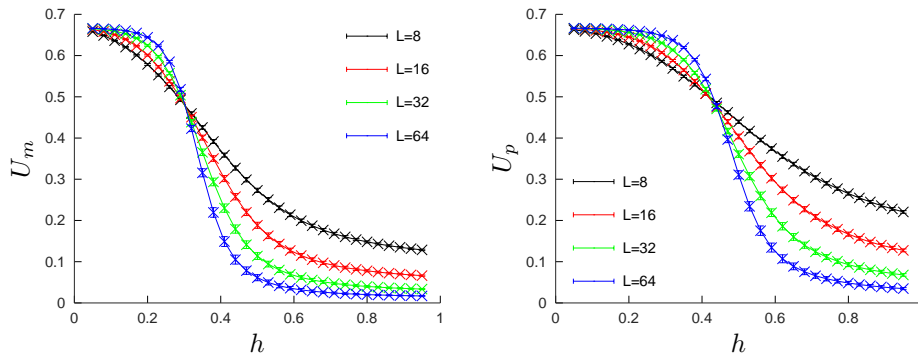


Figure 27. Average Binder cumulant of magnetization (left) and polarization (right) for the 2-color Ashkin-Teller model with $\epsilon = 2$. The data have been obtained using Algo. 3 with 4 states per site.

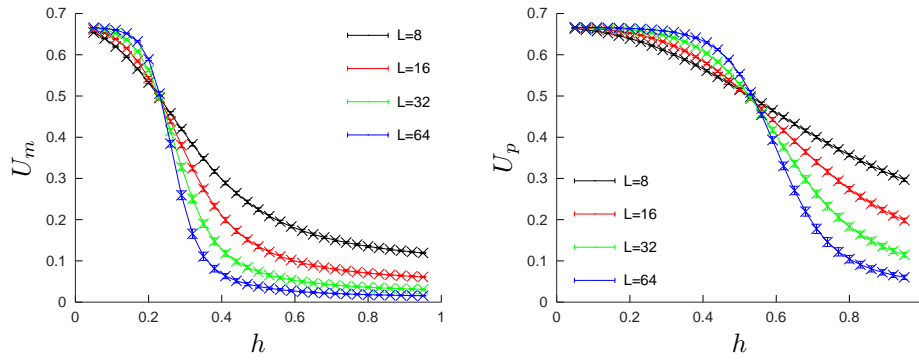


Figure 28. Average Binder cumulant of magnetization (left) and polarization (right) for the 2-color Ashkin-Teller model with $\epsilon = 2\sqrt{2}$. The data have been obtained using Algo. 3 with 4 states per site.

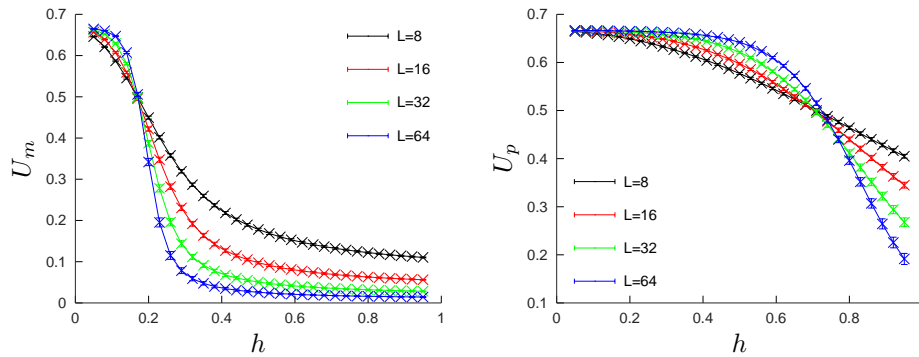


Figure 29. Average Binder cumulant of magnetization (left) and polarization (right) for the 2-color Ashkin-Teller model with $\epsilon = 4$. The data have been obtained using Algo. 3 with 4 states per site.

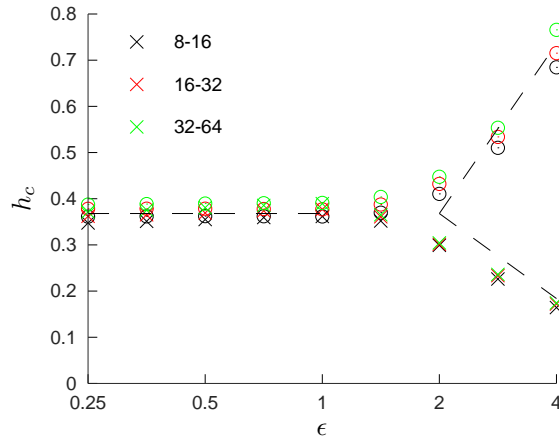


Figure 30. Phase diagram of the 2-color Ashkin-Teller model obtained from the crossings of the Binder cumulants U_m (crosses) and U_p (circles). The colors are associated to the pair of lattice sizes (see the legend) used to find the crossing of the cumulants. The data have been obtained using Algo. 3 with 4 states per site.

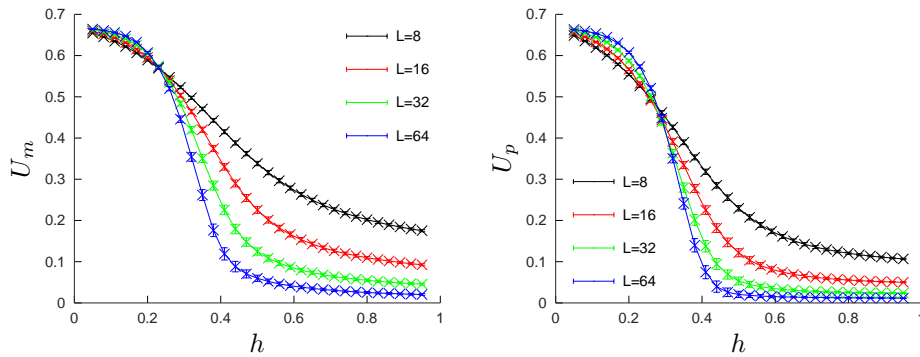


Figure 31. Average Binder cumulant of magnetization (left) and polarization (right) for the 2-color Ashkin-Teller model with $\epsilon = 1/4$. The data have been obtained using Algo. 1 with 8 states per site.

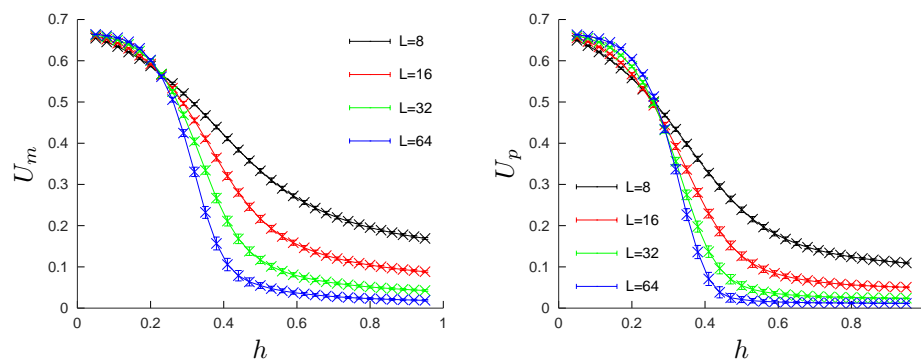


Figure 32. Average Binder cumulant of magnetization (left) and polarization (right) for the 2-color Ashkin-Teller model with $\epsilon = \sqrt{2}/4$. The data have been obtained using Algo. 1 with 8 states per site.

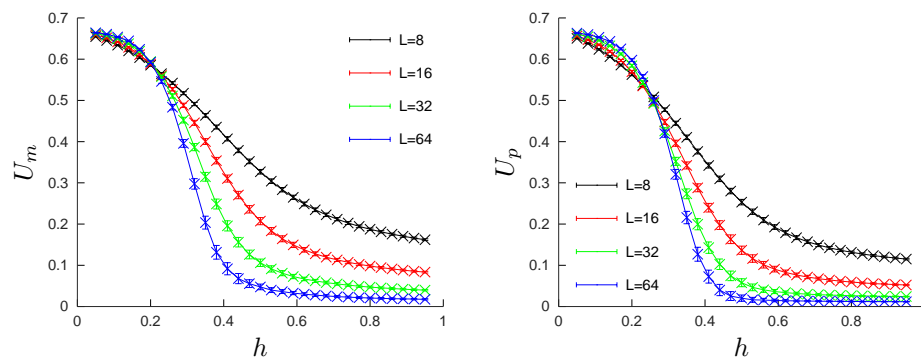


Figure 33. Average Binder cumulant of magnetization (left) and polarization (right) for the 2-color Ashkin-Teller model with $\epsilon = 1/2$. The data have been obtained using Algo. 1 with 8 states per site.

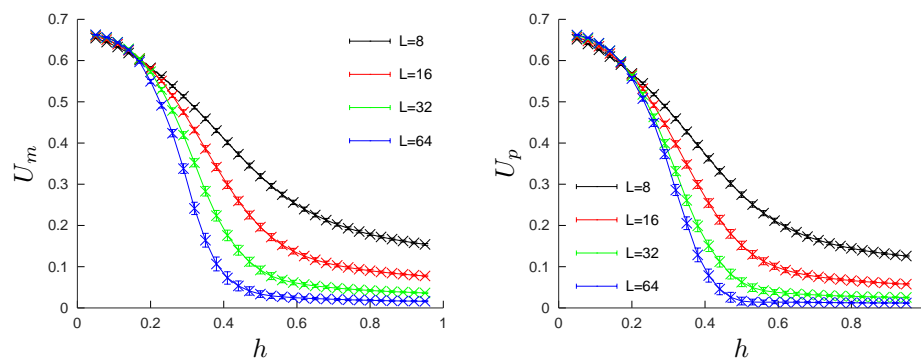


Figure 34. Average Binder cumulant of magnetization (left) and polarization (right) for the 2-color Ashkin-Teller model with $\epsilon = \sqrt{2}/2$. The data have been obtained using Algo. 1 with 8 states per site.

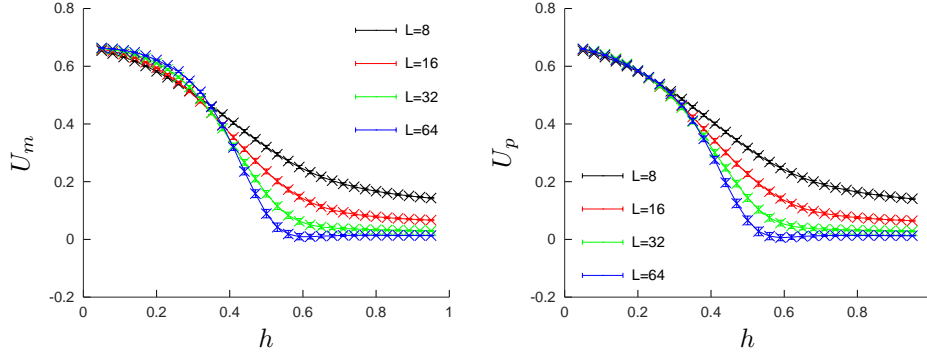


Figure 35. Average Binder cumulant of magnetization (left) and polarization (right) for the 2-color Ashkin-Teller model with $\epsilon = 1$. The data have been obtained using Algo. 1 with 8 states per site.

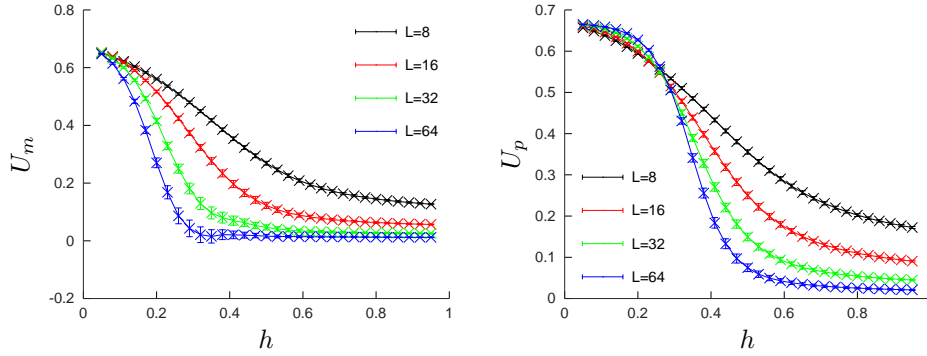


Figure 36. Average Binder cumulant of magnetization (left) and polarization (right) for the 2-color Ashkin-Teller model with $\epsilon = \sqrt{2}$. The data have been obtained using Algo. 1 with 8 states per site.

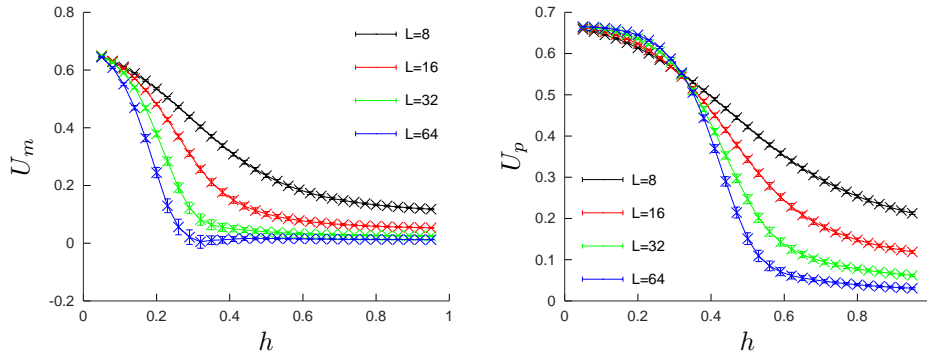


Figure 37. Average Binder cumulant of magnetization (left) and polarization (right) for the 2-color Ashkin-Teller model with $\epsilon = 2$. The data have been obtained using Algo. 1 with 8 states per site.

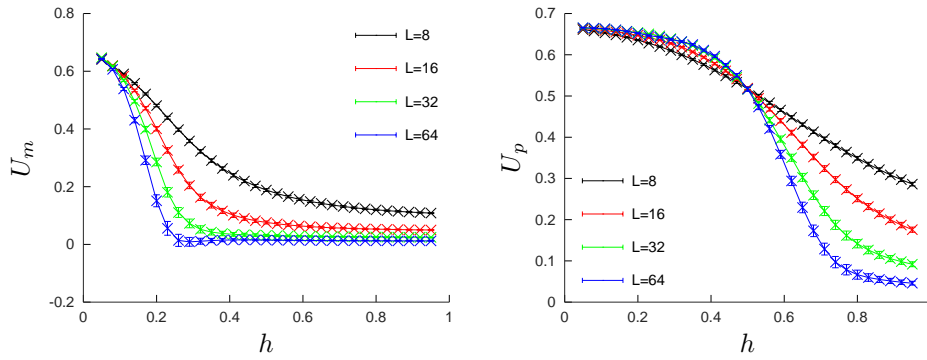


Figure 38. Average Binder cumulant of magnetization (left) and polarization (right) for the 2-color Ashkin-Teller model with $\epsilon = 2\sqrt{2}$. The data have been obtained using Algo. 1 with 8 states per site.

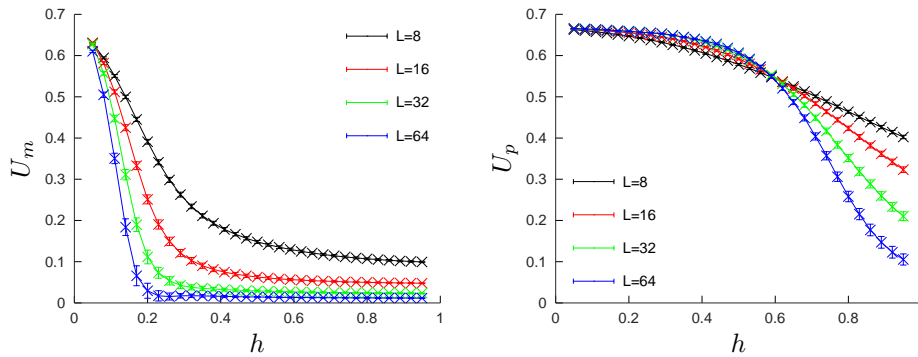


Figure 39. Average Binder cumulant of magnetization (left) and polarization (right) for the 2-color Ashkin-Teller model with $\epsilon = 4$. The data have been obtained using Algo. 1 with 8 states per site.

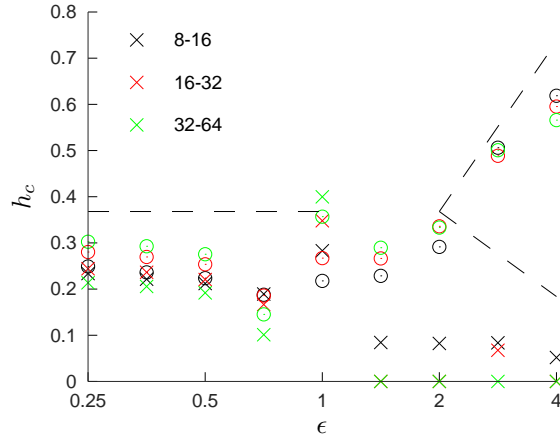


Figure 40. Phase diagram of the 2-color Ashkin-Teller model obtained from the crossings of the Binder cumulants U_m (crosses) and U_p (circles). The colors are associated to the pair of lattice sizes (see the legend) used to find the crossing of the cumulants. The data have been obtained using Algo. 1 with 8 states per site.

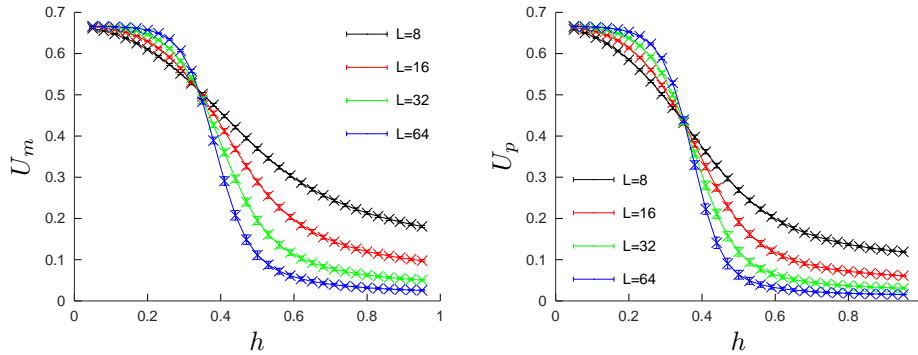


Figure 41. Average Binder cumulant of magnetization (left) and polarization (right) for the 2-color Ashkin-Teller model with $\epsilon = 1/4$. The data have been obtained using Algo. 2 with 8 states per site.

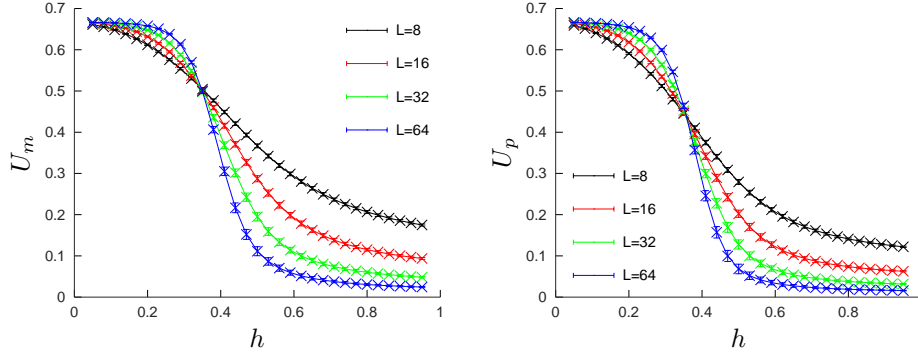


Figure 42. Average Binder cumulant of magnetization (left) and polarization (right) for the 2-color Ashkin-Teller model with $\epsilon = \sqrt{2}/4$. The data have been obtained using Algo. 2 with 8 states per site.

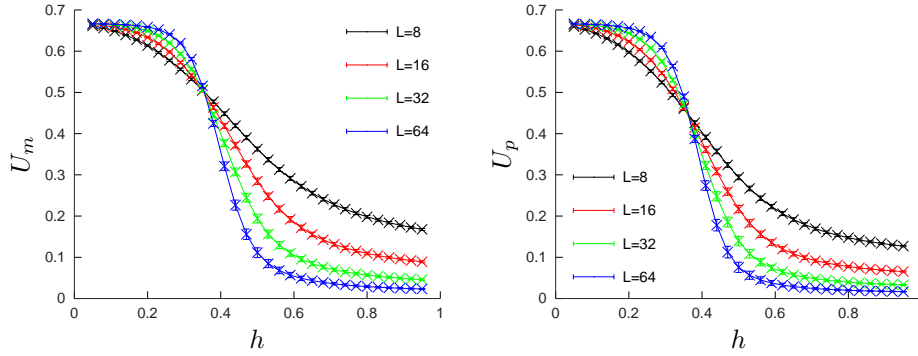


Figure 43. Average Binder cumulant of magnetization (left) and polarization (right) for the 2-color Ashkin-Teller model with $\epsilon = 1/2$. The data have been obtained using Algo. 2 with 8 states per site.

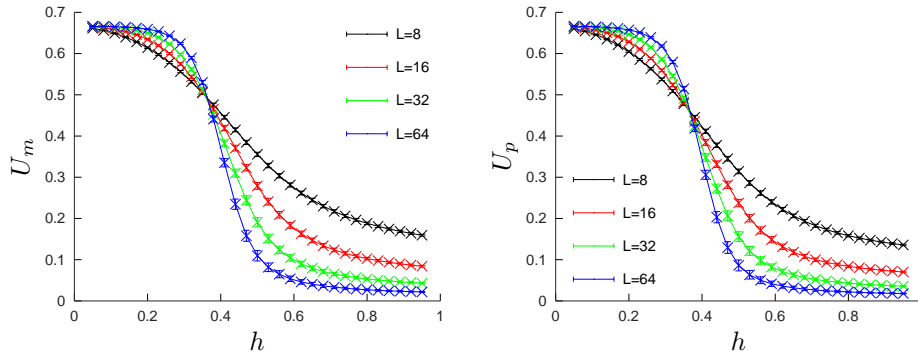


Figure 44. Average Binder cumulant of magnetization (left) and polarization (right) for the 2-color Ashkin-Teller model with $\epsilon = \sqrt{2}/2$. The data have been obtained using Algo. 2 with 8 states per site.

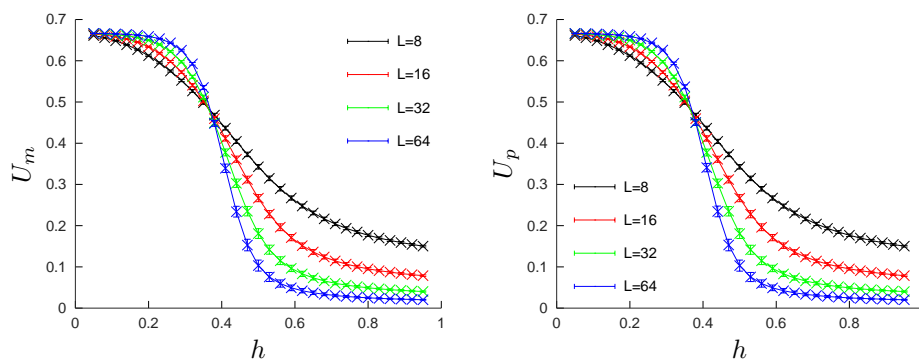


Figure 45. Average Binder cumulant of magnetization (left) and polarization (right) for the 2-color Ashkin-Teller model with $\epsilon = 1$. The data have been obtained using Algo. 2 with 8 states per site.

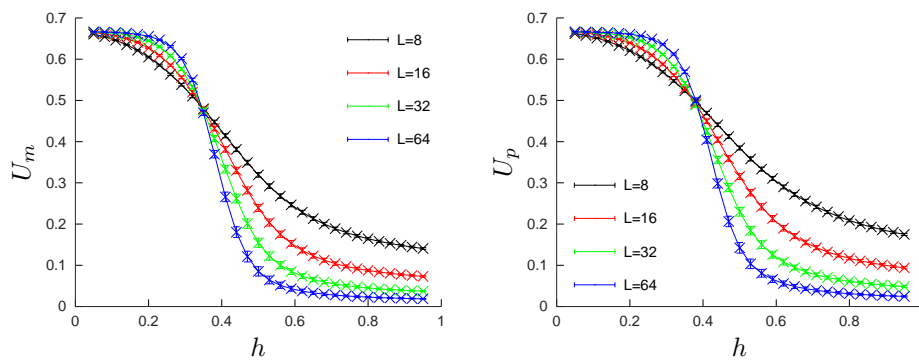


Figure 46. Average Binder cumulant of magnetization (left) and polarization (right) for the 2-color Ashkin-Teller model with $\epsilon = \sqrt{2}$. The data have been obtained using Algo. 2 with 8 states per site.

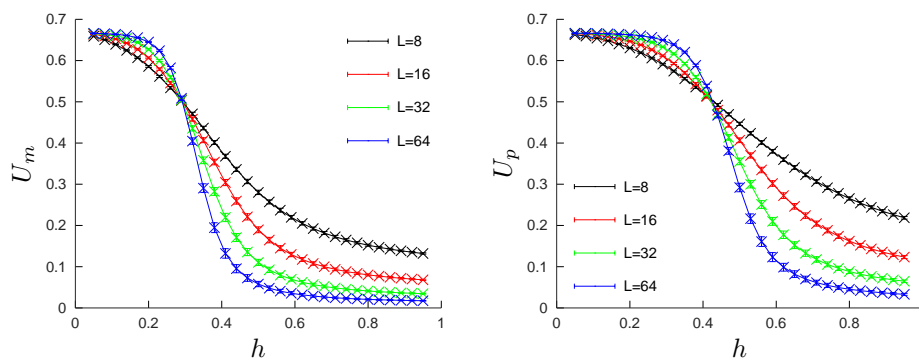


Figure 47. Average Binder cumulant of magnetization (left) and polarization (right) for the 2-color Ashkin-Teller model with $\epsilon = 2$. The data have been obtained using Algo. 2 with 8 states per site.

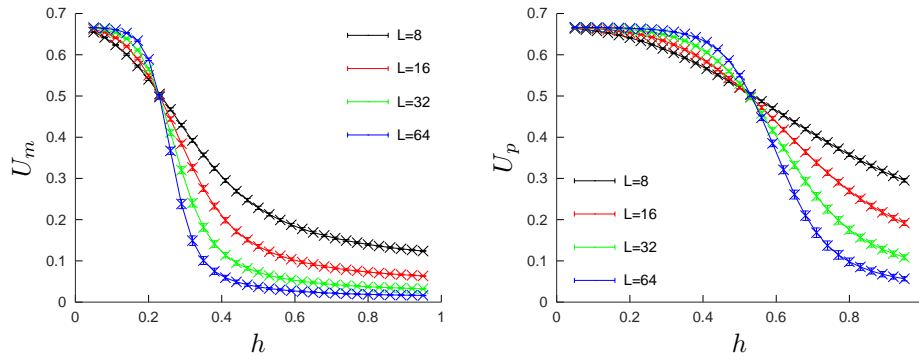


Figure 48. Average Binder cumulant of magnetization (left) and polarization (right) for the 2-color Ashkin-Teller model with $\epsilon = 2\sqrt{2}$. The data have been obtained using Algo. 2 with 8 states per site.

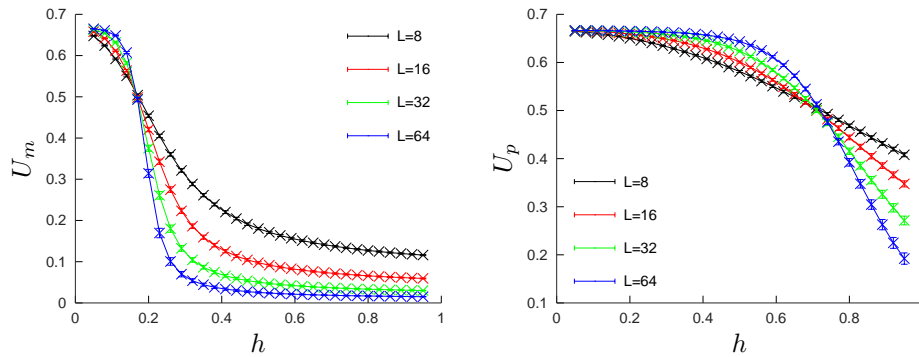


Figure 49. Average Binder cumulant of magnetization (left) and polarization (right) for the 2-color Ashkin-Teller model with $\epsilon = 4$. The data have been obtained using Algo. 2 with 8 states per site.

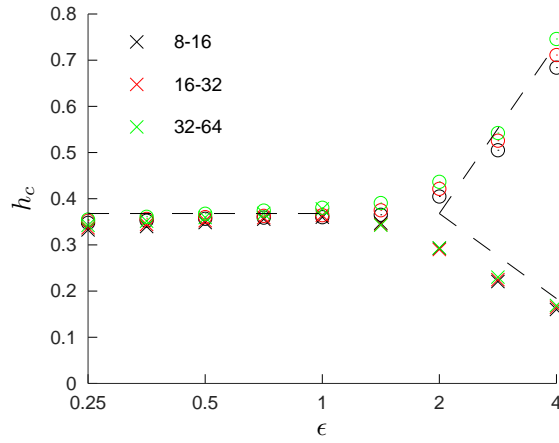


Figure 50. Phase diagram of the 2-color Ashkin-Teller model obtained from the crossings of the Binder cumulants U_m (crosses) and U_p (circles). The colors are associated to the pair of lattice sizes (see the legend) used to find the crossing of the cumulants. The data have been obtained using Algo. 2 with 8 states per site.

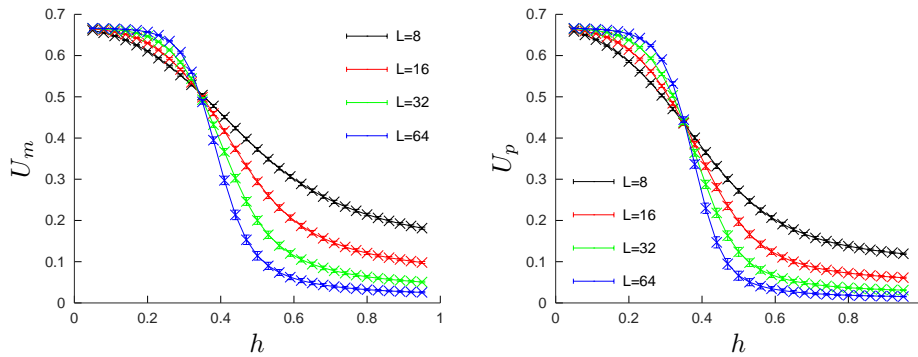


Figure 51. Average Binder cumulant of magnetization (left) and polarization (right) for the 2-color Ashkin-Teller model with $\epsilon = 1/4$. The data have been obtained using Algo. 3 with 8 states per site.

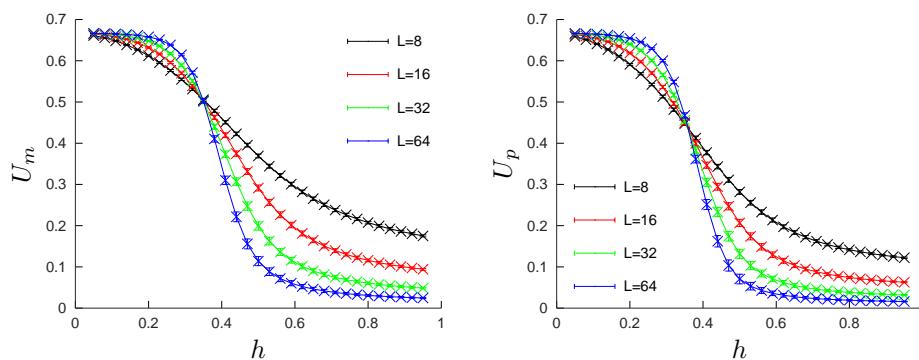


Figure 52. Average Binder cumulant of magnetization (left) and polarization (right) for the 2-color Ashkin-Teller model with $\epsilon = \sqrt{2}/4$. The data have been obtained using Algo. 3 with 8 states per site.

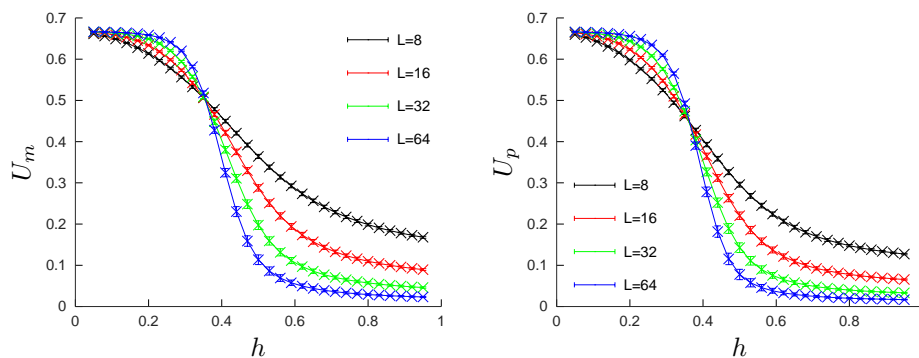


Figure 53. Average Binder cumulant of magnetization (left) and polarization (right) for the 2-color Ashkin-Teller model with $\epsilon = 1/2$. The data have been obtained using Algo. 3 with 8 states per site.

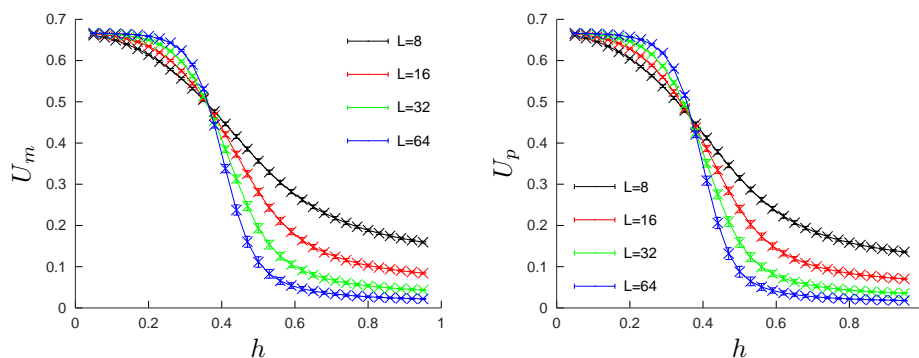


Figure 54. Average Binder cumulant of magnetization (left) and polarization (right) for the 2-color Ashkin-Teller model with $\epsilon = \sqrt{2}/2$. The data have been obtained using Algo. 3 with 8 states per site.

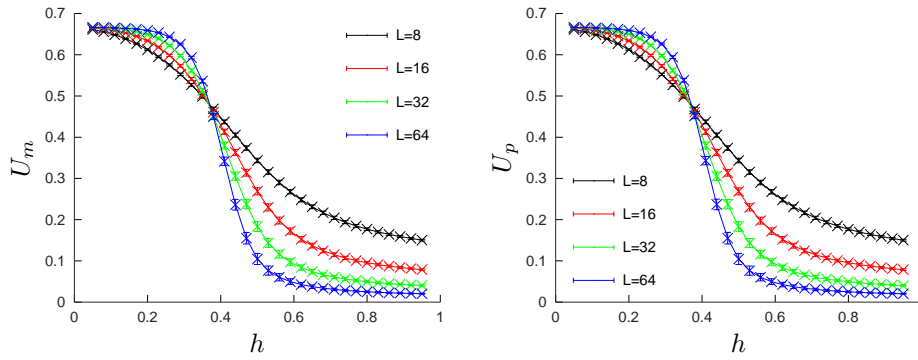


Figure 55. Average Binder cumulant of magnetization (left) and polarization (right) for the 2-color Ashkin-Teller model with $\epsilon = 1$. The data have been obtained using Algo. 3 with 8 states per site.

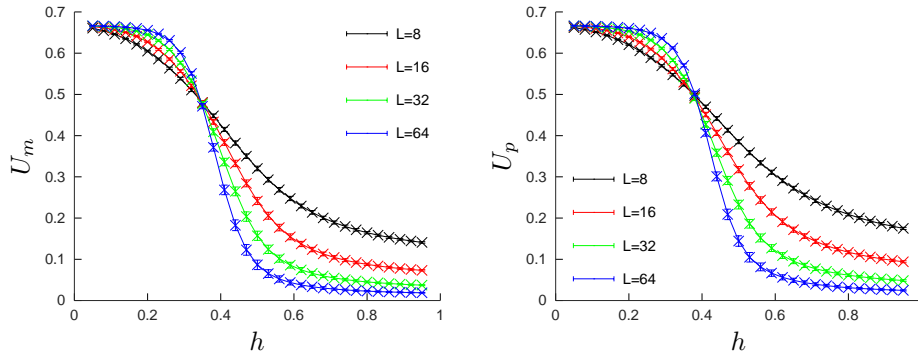


Figure 56. Average Binder cumulant of magnetization (left) and polarization (right) for the 2-color Ashkin-Teller model with $\epsilon = \sqrt{2}$. The data have been obtained using Algo. 3 with 8 states per site.

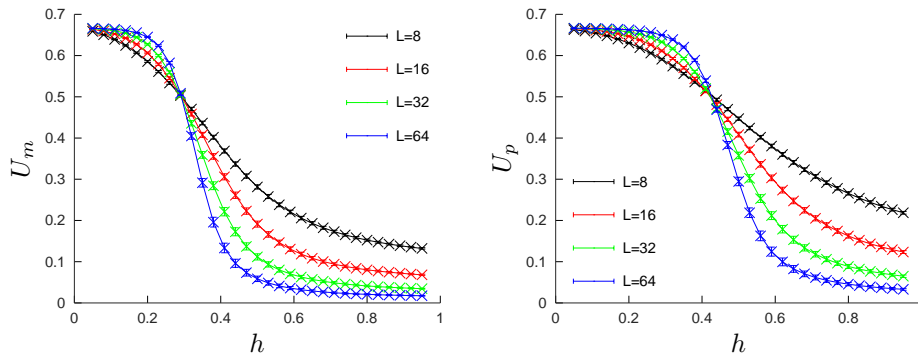


Figure 57. Average Binder cumulant of magnetization (left) and polarization (right) for the 2-color Ashkin-Teller model with $\epsilon = 2$. The data have been obtained using Algo. 3 with 8 states per site.

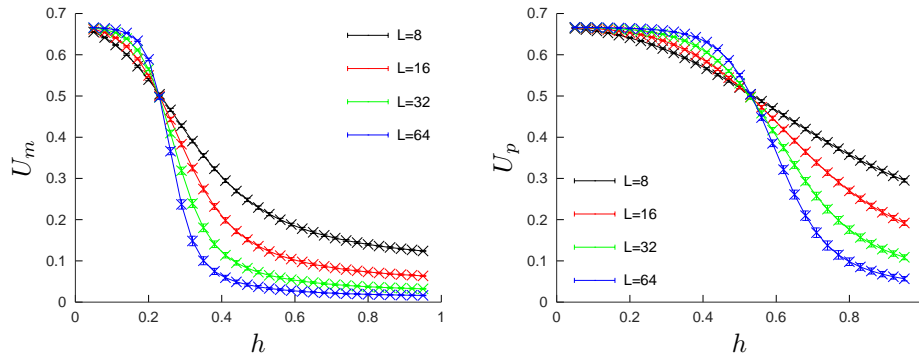


Figure 58. Average Binder cumulant of magnetization (left) and polarization (right) for the 2-color Ashkin-Teller model with $\epsilon = 2\sqrt{2}$. The data have been obtained using Algo. 3 with 8 states per site.

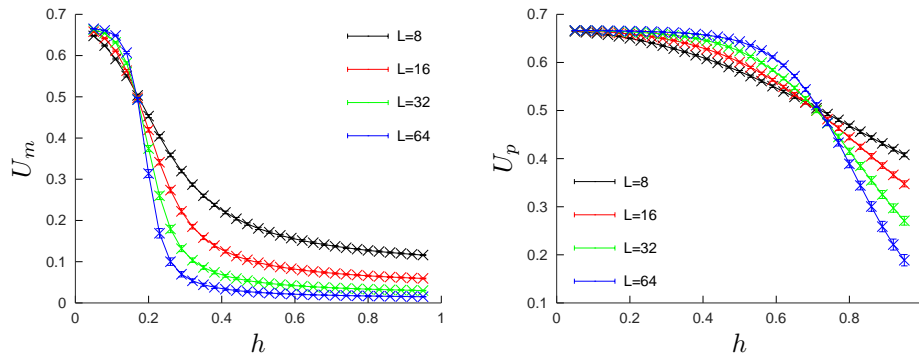


Figure 59. Average Binder cumulant of magnetization (left) and polarization (right) for the 2-color Ashkin-Teller model with $\epsilon = 4$. The data have been obtained using Algo. 3 with 8 states per site.

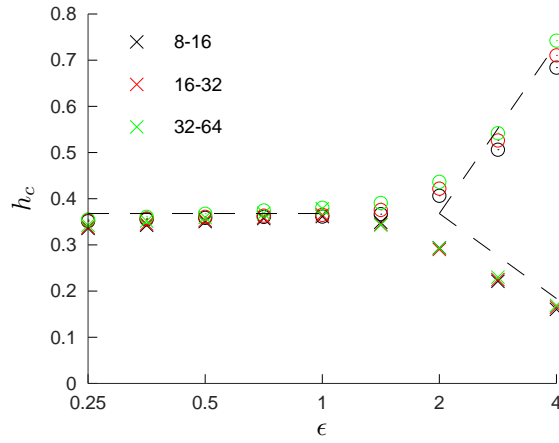


Figure 60. Phase diagram of the 2-color Ashkin-Teller model obtained from the crossings of the Binder cumulants U_m (crosses) and U_p (circles). The colors are associated to the pair of lattice sizes (see the legend) used to find the crossing of the cumulants. The data have been obtained using Algo. 3 with 8 states per site.

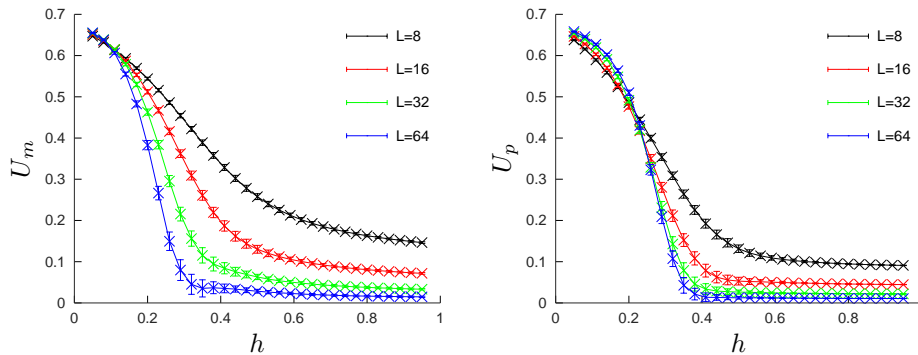


Figure 61. Average Binder cumulant of magnetization (left) and polarization (right) for the 3-color Ashkin-Teller model with $\epsilon = 1/4$. The data have been obtained using Algo. 1 with 8 states per site.

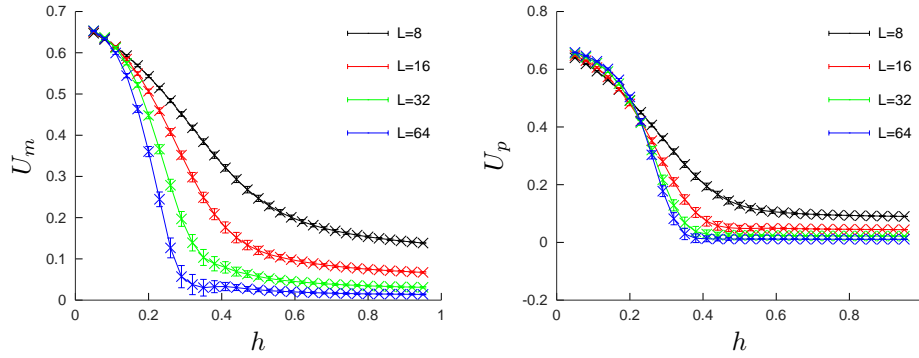


Figure 62. Average Binder cumulant of magnetization (left) and polarization (right) for the 3-color Ashkin-Teller model with $\epsilon = \sqrt{2}/4$. The data have been obtained using Algo. 1 with 8 states per site.

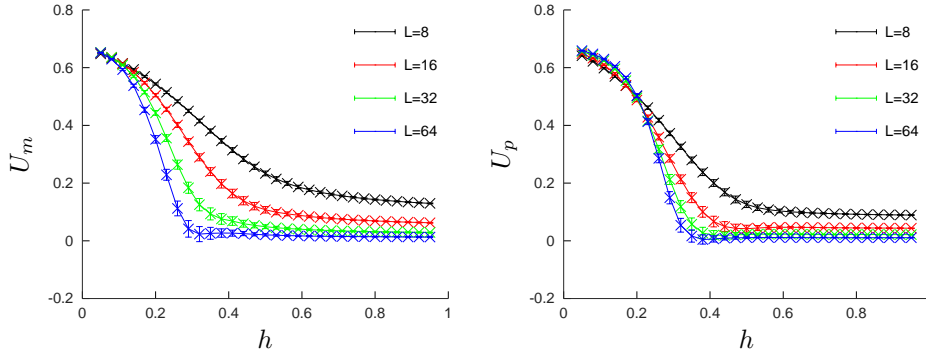


Figure 63. Average Binder cumulant of magnetization (left) and polarization (right) for the 3-color Ashkin-Teller model with $\epsilon = 1/2$. The data have been obtained using Algo. 1 with 8 states per site.

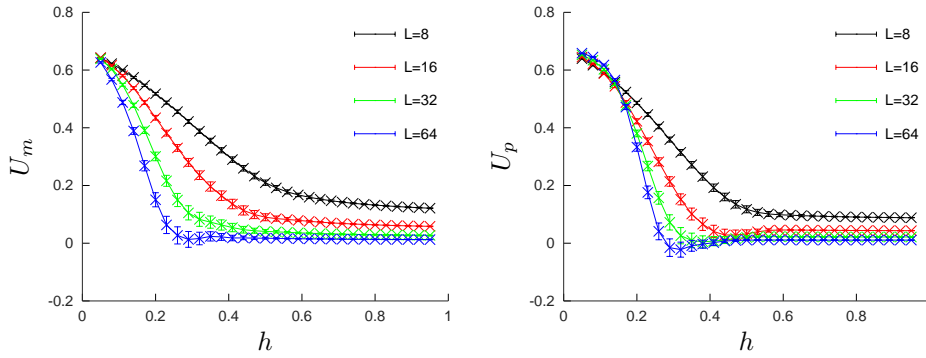


Figure 64. Average Binder cumulant of magnetization (left) and polarization (right) for the 3-color Ashkin-Teller model with $\epsilon = \sqrt{2}/2$. The data have been obtained using Algo. 1 with 8 states per site.

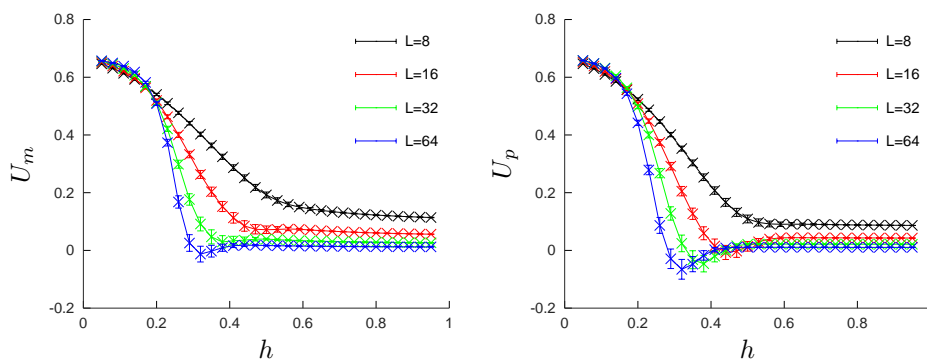


Figure 65. Average Binder cumulant of magnetization (left) and polarization (right) for the 3-color Ashkin-Teller model with $\epsilon = 1$. The data have been obtained using Algo. 1 with 8 states per site.

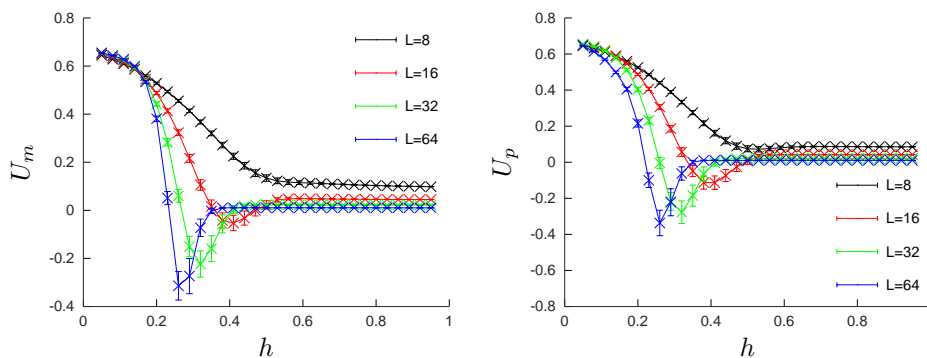


Figure 66. Average Binder cumulant of magnetization (left) and polarization (right) for the 3-color Ashkin-Teller model with $\epsilon = \sqrt{2}$. The data have been obtained using Algo. 1 with 8 states per site.

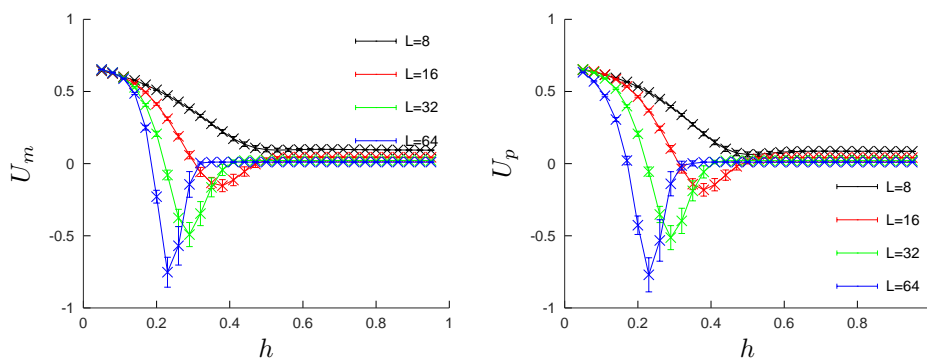


Figure 67. Average Binder cumulant of magnetization (left) and polarization (right) for the 3-color Ashkin-Teller model with $\epsilon = 2$. The data have been obtained using Algo. 1 with 8 states per site.

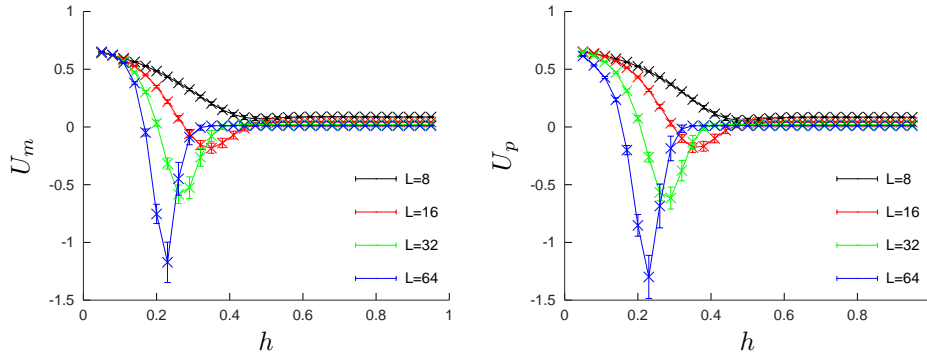


Figure 68. Average Binder cumulant of magnetization (left) and polarization (right) for the 3-color Ashkin-Teller model with $\epsilon = 2\sqrt{2}$. The data have been obtained using Algo. 1 with 8 states per site.

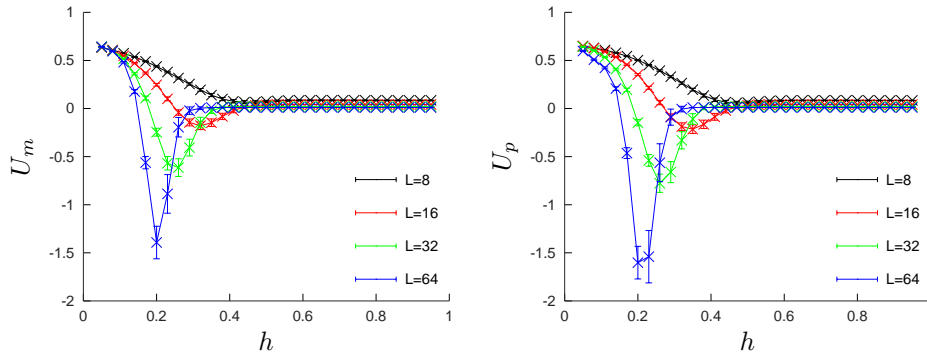


Figure 69. Average Binder cumulant of magnetization (left) and polarization (right) for the 3-color Ashkin-Teller model with $\epsilon = 4$. The data have been obtained using Algo. 1 with 8 states per site.

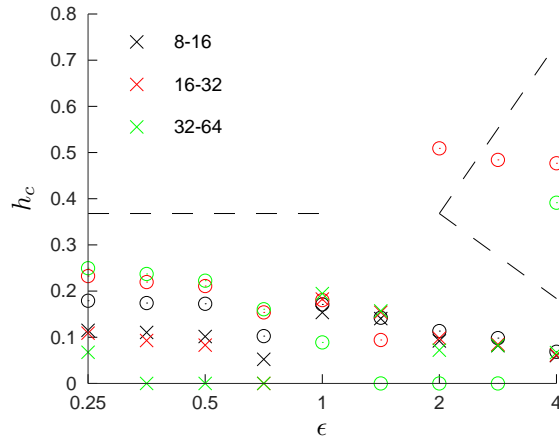


Figure 70. Phase diagram of the 3-color Ashkin-Teller model obtained from the crossings of the Binder cumulants U_m (crosses) and U_p (circles). The colors are associated to the pair of lattice sizes (see the legend) used to find the crossing of the cumulants. The data have been obtained using Algo. 1 with 8 states per site.

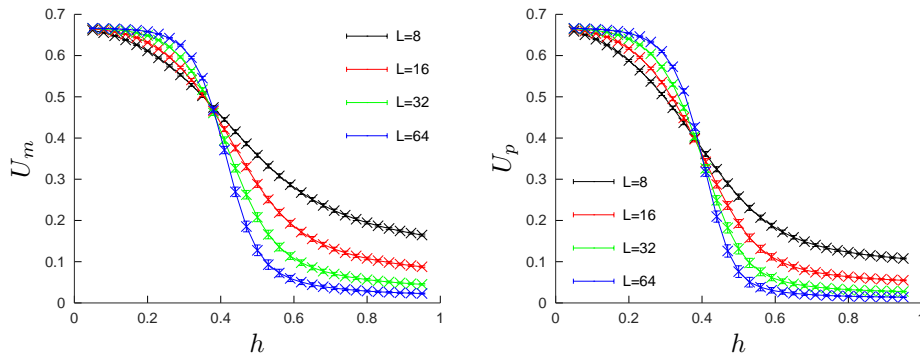


Figure 71. Average Binder cumulant of magnetization (left) and polarization (right) for the 3-color Ashkin-Teller model with $\epsilon = 1/4$. The data have been obtained using Algo. 2 with 8 states per site.

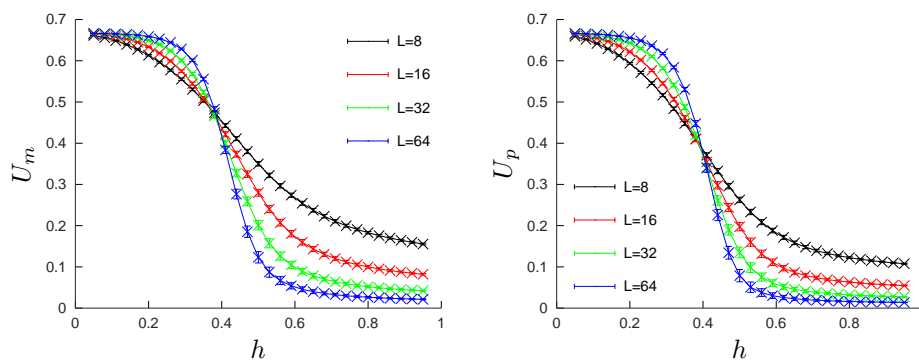


Figure 72. Average Binder cumulant of magnetization (left) and polarization (right) for the 3-color Ashkin-Teller model with $\epsilon = \sqrt{2}/4$. The data have been obtained using Algo. 2 with 8 states per site.

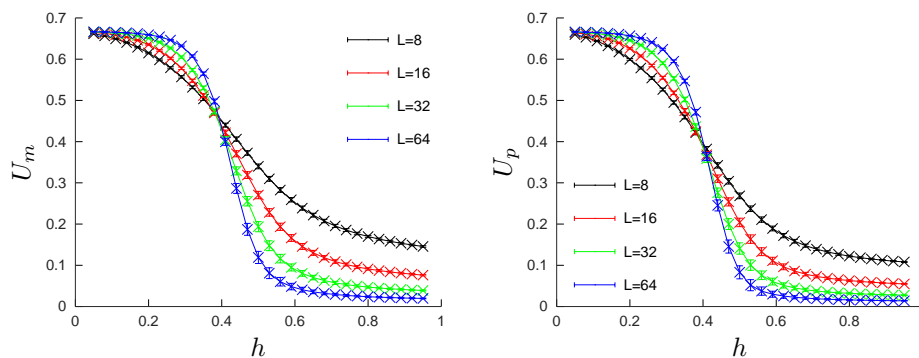


Figure 73. Average Binder cumulant of magnetization (left) and polarization (right) for the 3-color Ashkin-Teller model with $\epsilon = 1/2$. The data have been obtained using Algo. 2 with 8 states per site.

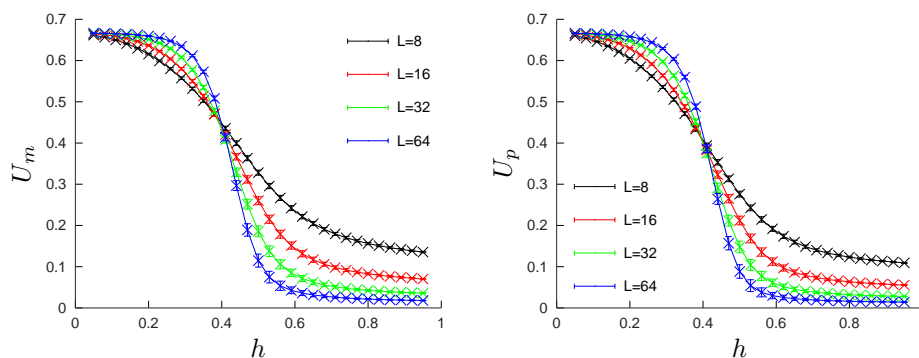


Figure 74. Average Binder cumulant of magnetization (left) and polarization (right) for the 3-color Ashkin-Teller model with $\epsilon = \sqrt{2}/2$. The data have been obtained using Algo. 2 with 8 states per site.

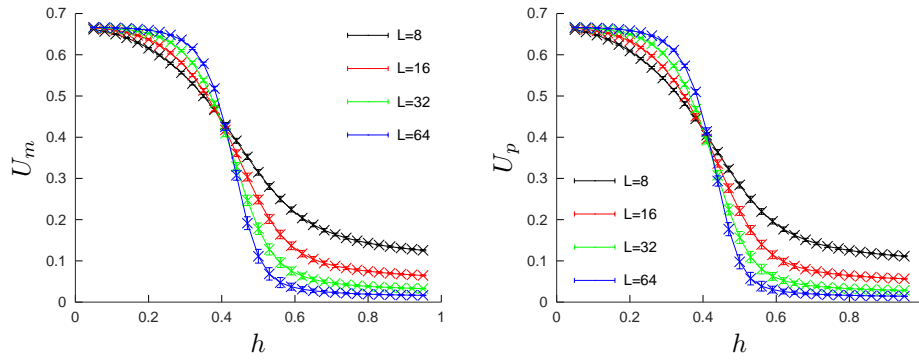


Figure 75. Average Binder cumulant of magnetization (left) and polarization (right) for the 3-color Ashkin-Teller model with $\epsilon = 1$. The data have been obtained using Algo. 2 with 8 states per site.

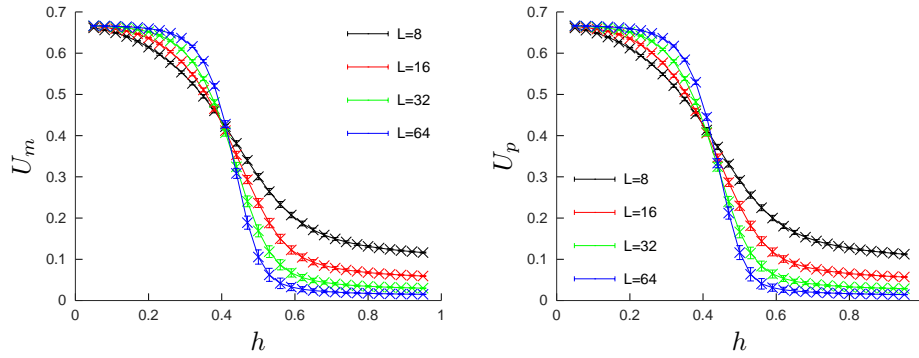


Figure 76. Average Binder cumulant of magnetization (left) and polarization (right) for the 3-color Ashkin-Teller model with $\epsilon = \sqrt{2}$. The data have been obtained using Algo. 2 with 8 states per site.

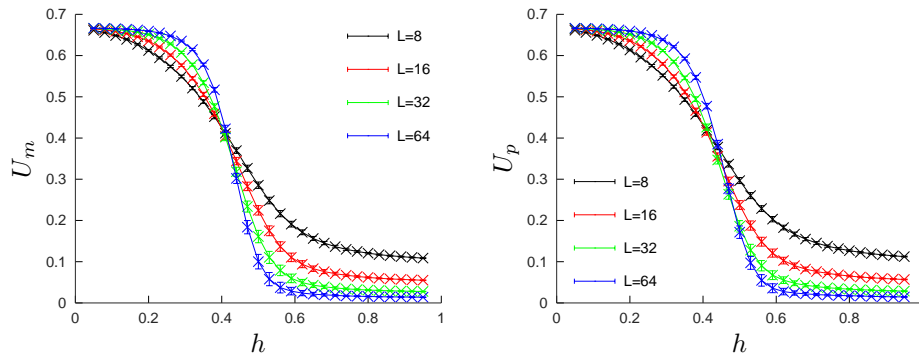


Figure 77. Average Binder cumulant of magnetization (left) and polarization (right) for the 3-color Ashkin-Teller model with $\epsilon = 2$. The data have been obtained using Algo. 2 with 8 states per site.

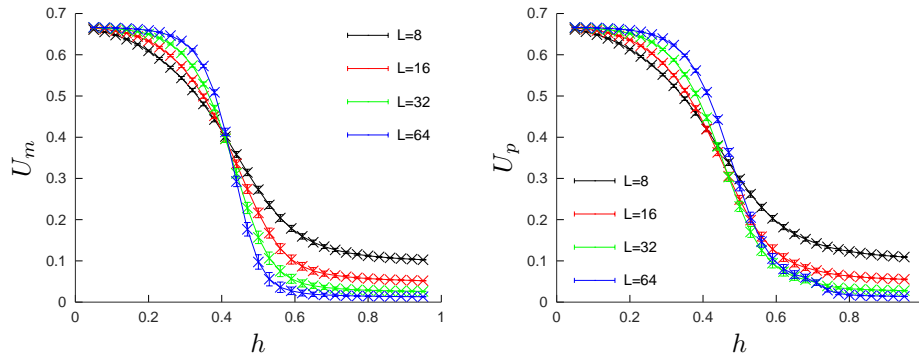


Figure 78. Average Binder cumulant of magnetization (left) and polarization (right) for the 3-color Ashkin-Teller model with $\epsilon = 2\sqrt{2}$. The data have been obtained using Algo. 2 with 8 states per site.

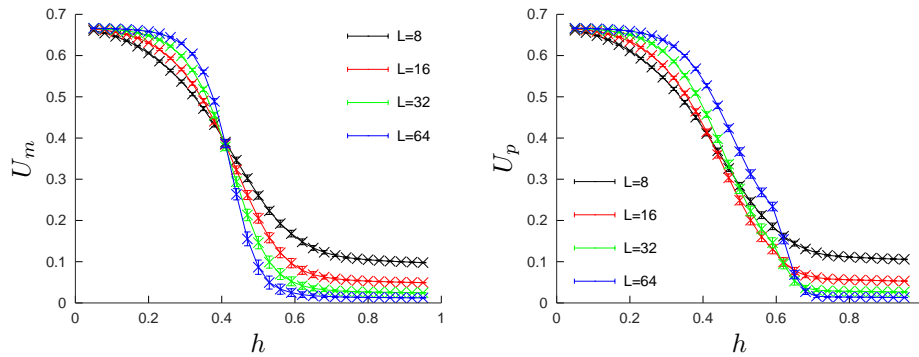


Figure 79. Average Binder cumulant of magnetization (left) and polarization (right) for the 3-color Ashkin-Teller model with $\epsilon = 4$. The data have been obtained using Algo. 2 with 8 states per site.

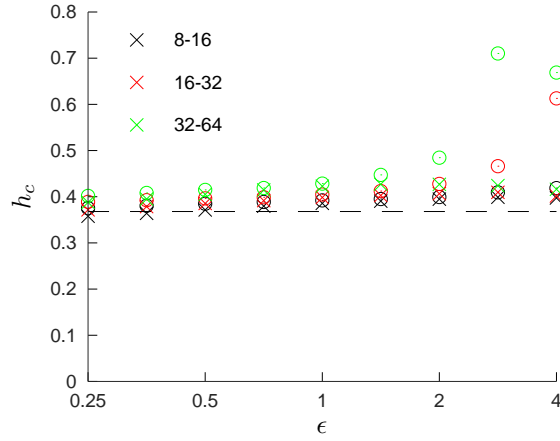


Figure 80. Phase diagram of the 3-color Ashkin-Teller model obtained from the crossings of the Binder cumulants U_m (crosses) and U_p (circles). The colors are associated to the pair of lattice sizes (see the legend) used to find the crossing of the cumulants. The data have been obtained using Algo. 2 with 8 states per site.

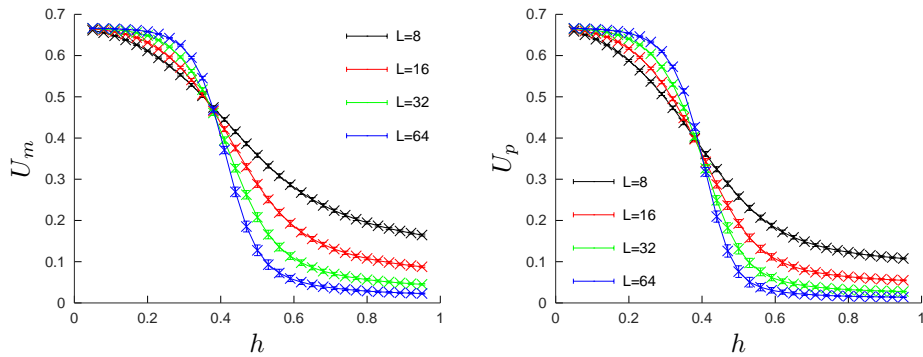


Figure 81. Average Binder cumulant of magnetization (left) and polarization (right) for the 3-color Ashkin-Teller model with $\epsilon = 1/4$. The data have been obtained using Algo. 3 with 8 states per site.

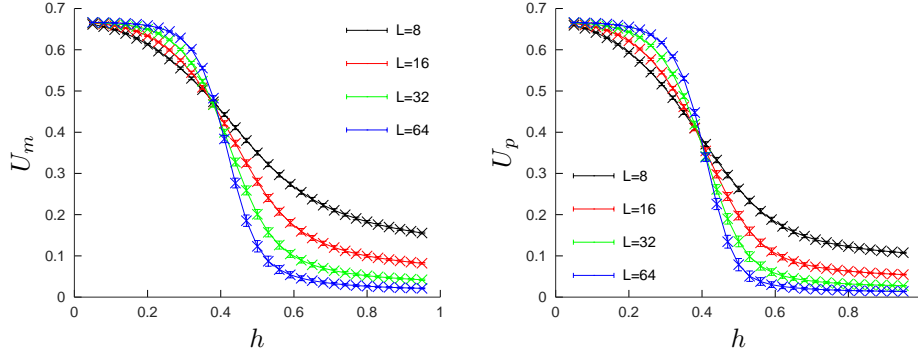


Figure 82. Average Binder cumulant of magnetization (left) and polarization (right) for the 3-color Ashkin-Teller model with $\epsilon = \sqrt{2}/4$. The data have been obtained using Algo. 3 with 8 states per site.

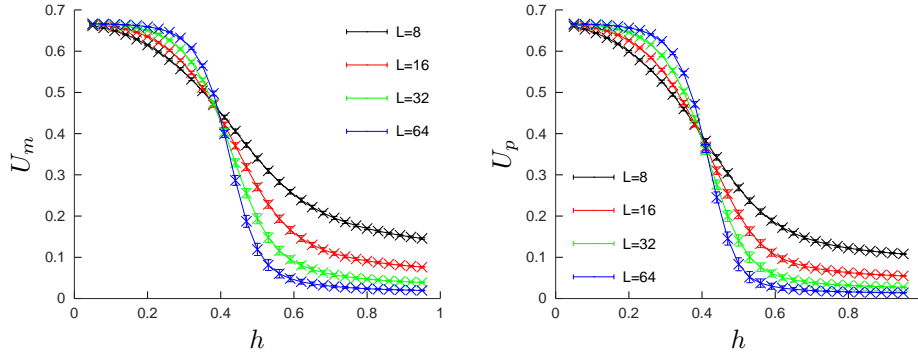


Figure 83. Average Binder cumulant of magnetization (left) and polarization (right) for the 3-color Ashkin-Teller model with $\epsilon = 1/2$. The data have been obtained using Algo. 3 with 8 states per site.

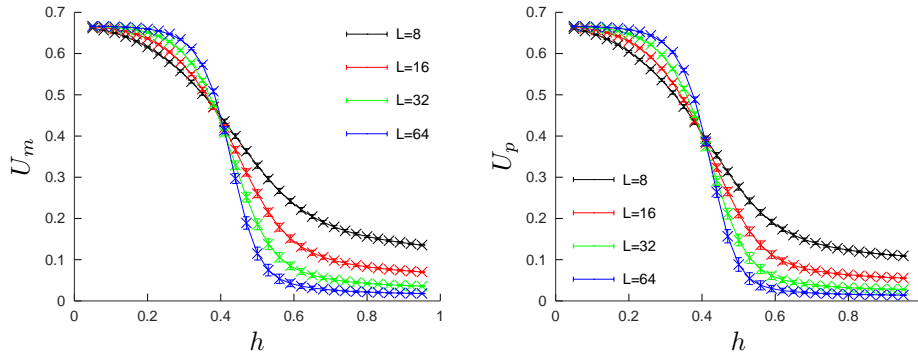


Figure 84. Average Binder cumulant of magnetization (left) and polarization (right) for the 3-color Ashkin-Teller model with $\epsilon = \sqrt{2}/2$. The data have been obtained using Algo. 3 with 8 states per site.

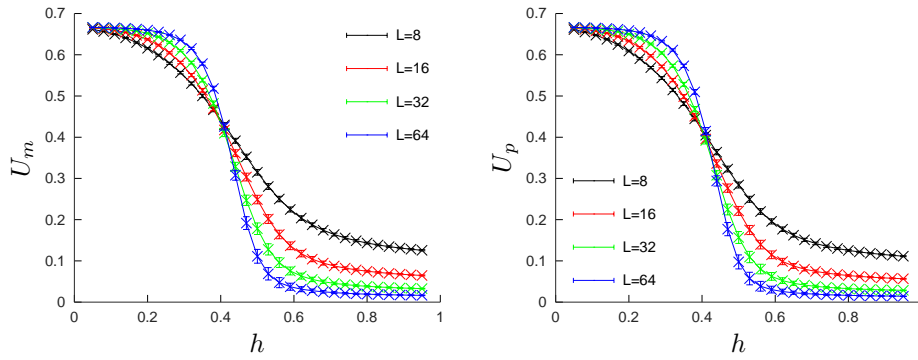


Figure 85. Average Binder cumulant of magnetization (left) and polarization (right) for the 3-color Ashkin-Teller model with $\epsilon = 1$. The data have been obtained using Algo. 3 with 8 states per site.

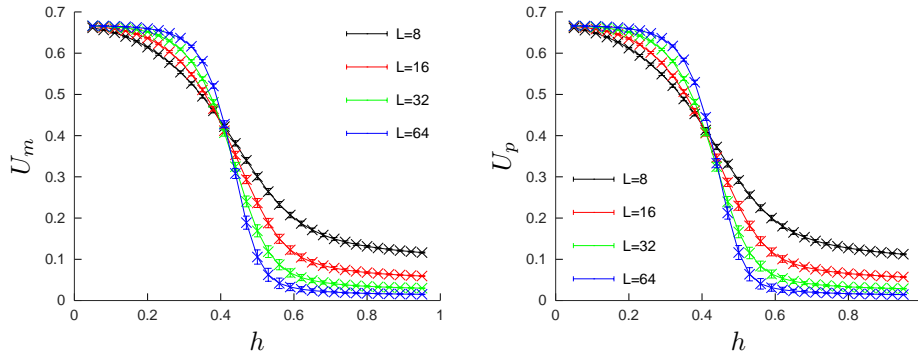


Figure 86. Average Binder cumulant of magnetization (left) and polarization (right) for the 3-color Ashkin-Teller model with $\epsilon = \sqrt{2}$. The data have been obtained using Algo. 3 with 8 states per site.

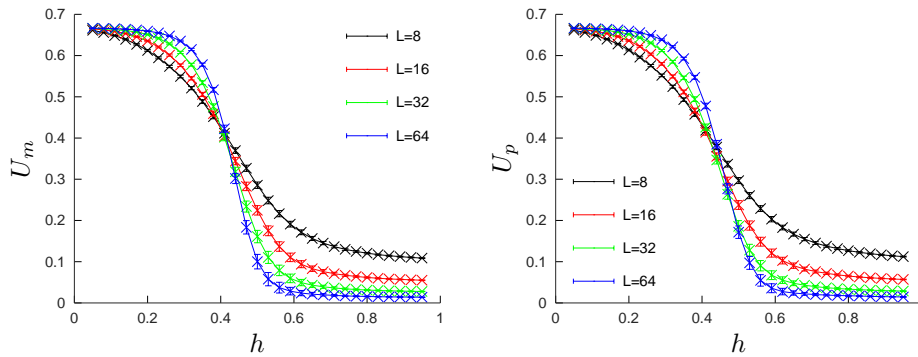


Figure 87. Average Binder cumulant of magnetization (left) and polarization (right) for the 3-color Ashkin-Teller model with $\epsilon = 2$. The data have been obtained using Algo. 3 with 8 states per site.

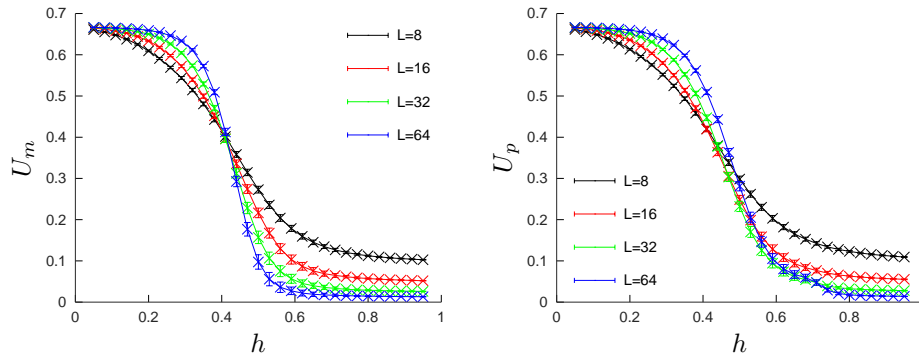


Figure 88. Average Binder cumulant of magnetization (left) and polarization (right) for the 3-color Ashkin-Teller model with $\epsilon = 2\sqrt{2}$. The data have been obtained using Algo. 3 with 8 states per site.

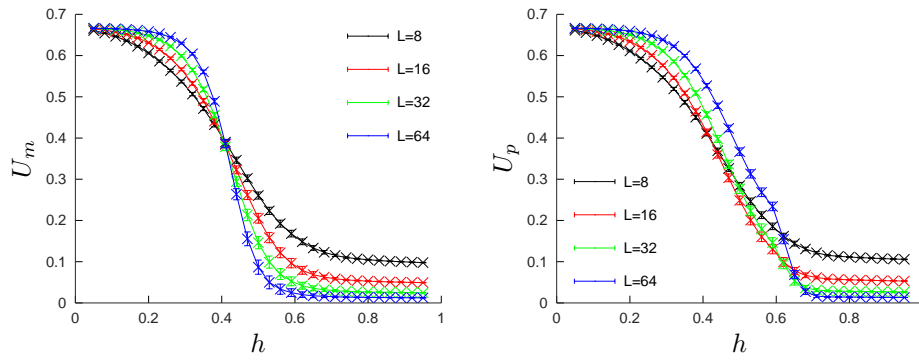


Figure 89. Average Binder cumulant of magnetization (left) and polarization (right) for the 3-color Ashkin-Teller model with $\epsilon = 4$. The data have been obtained using Algo. 3 with 8 states per site.

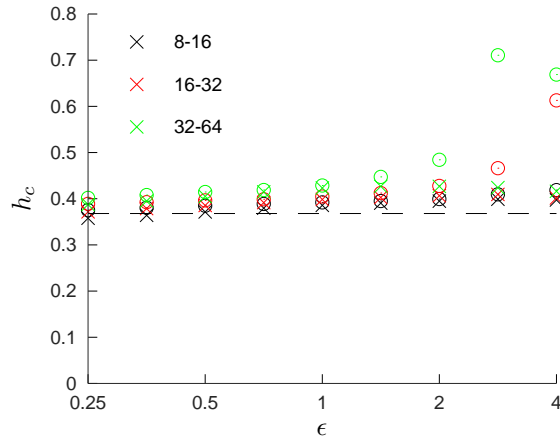


Figure 90. Phase diagram of the 3-color Ashkin-Teller model obtained from the crossings of the Binder cumulants U_m (crosses) and U_p (circles). The colors are associated to the pair of lattice sizes (see the legend) used to find the crossing of the cumulants. The data have been obtained using Algo. 3 with 8 states per site.

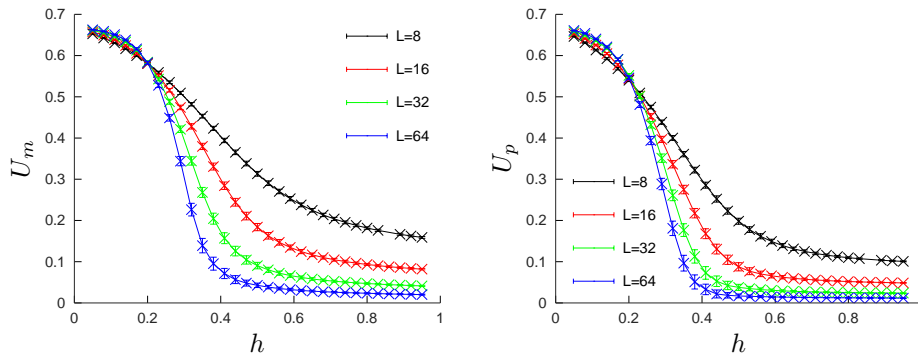


Figure 91. Average Binder cumulant of magnetization (left) and polarization (right) for the 3-color Ashkin-Teller model with $\epsilon = 1/4$. The data have been obtained using Algo. 1 with 16 states per site.

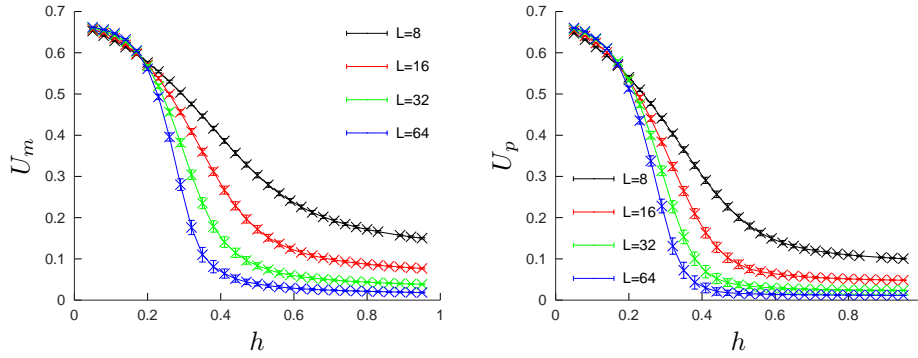


Figure 92. Average Binder cumulant of magnetization (left) and polarization (right) for the 3-color Ashkin-Teller model with $\epsilon = \sqrt{2}/4$. The data have been obtained using Algo. 1 with 16 states per site.

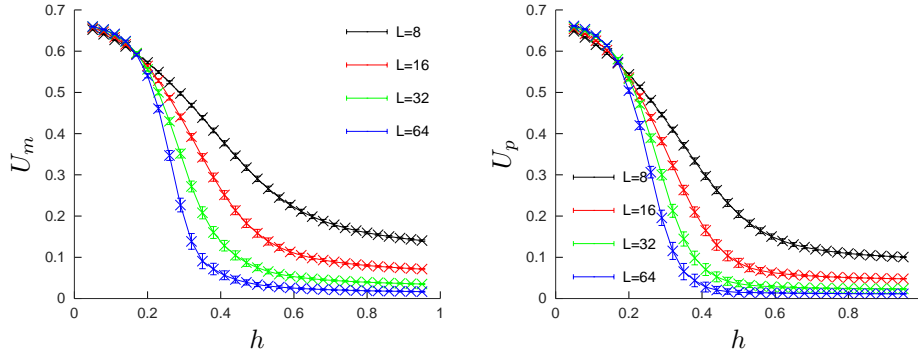


Figure 93. Average Binder cumulant of magnetization (left) and polarization (right) for the 3-color Ashkin-Teller model with $\epsilon = 1/2$. The data have been obtained using Algo. 1 with 16 states per site.

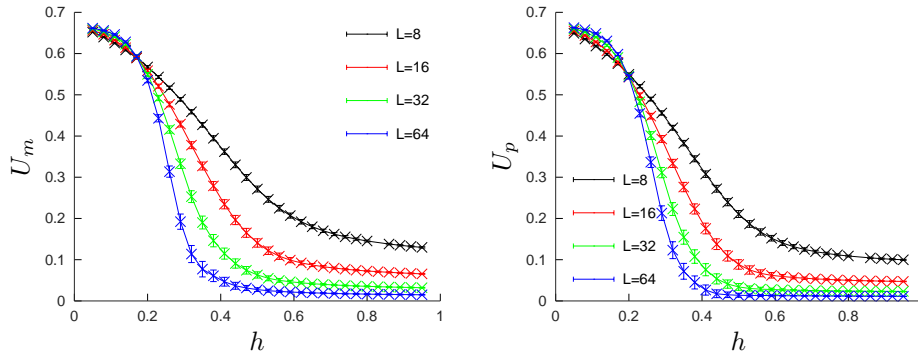


Figure 94. Average Binder cumulant of magnetization (left) and polarization (right) for the 3-color Ashkin-Teller model with $\epsilon = \sqrt{2}/2$. The data have been obtained using Algo. 1 with 16 states per site.

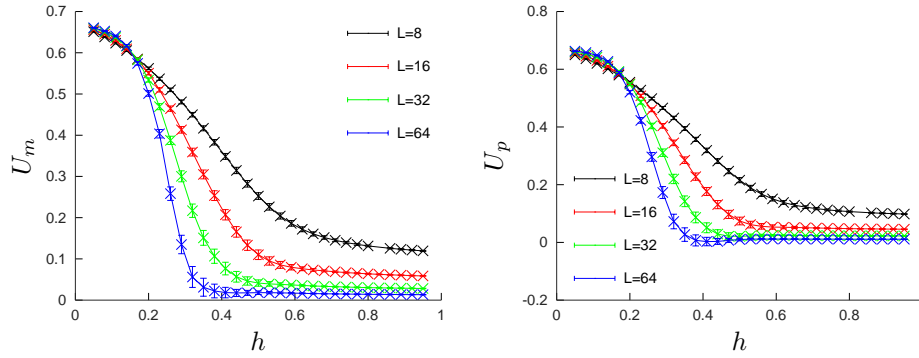


Figure 95. Average Binder cumulant of magnetization (left) and polarization (right) for the 3-color Ashkin-Teller model with $\epsilon = 1$. The data have been obtained using Algo. 1 with 16 states per site.

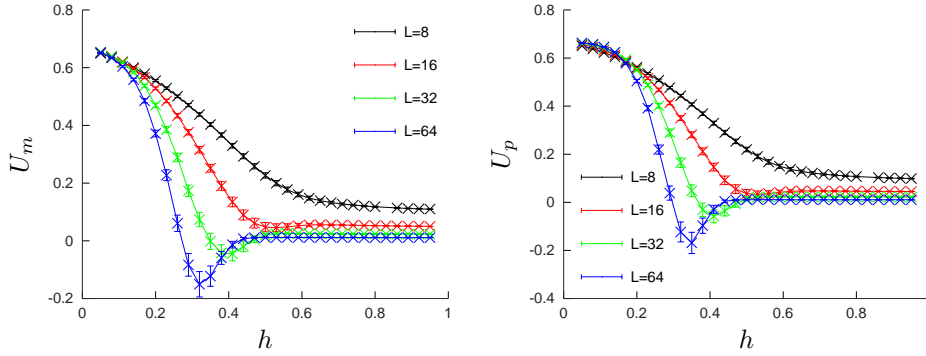


Figure 96. Average Binder cumulant of magnetization (left) and polarization (right) for the 3-color Ashkin-Teller model with $\epsilon = \sqrt{2}$. The data have been obtained using Algo. 1 with 16 states per site.

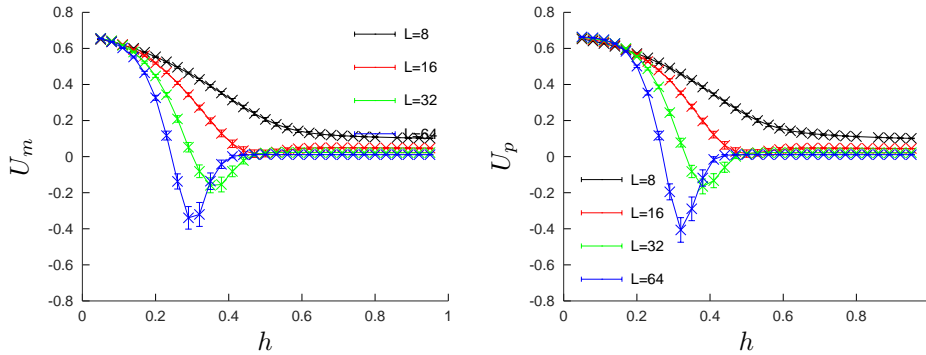


Figure 97. Average Binder cumulant of magnetization (left) and polarization (right) for the 3-color Ashkin-Teller model with $\epsilon = 2$. The data have been obtained using Algo. 1 with 16 states per site.

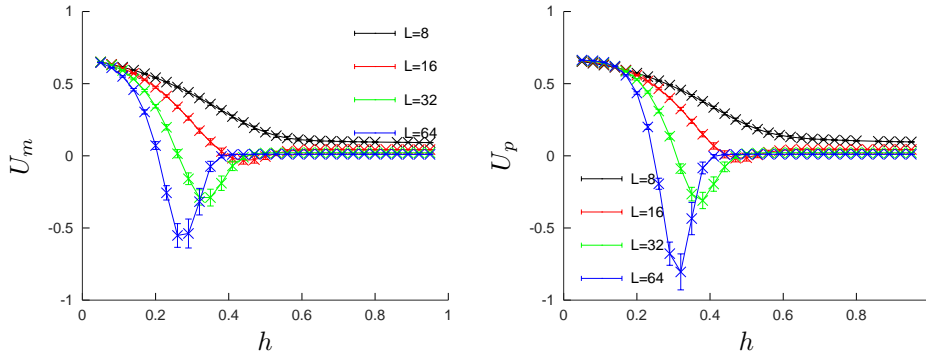


Figure 98. Average Binder cumulant of magnetization (left) and polarization (right) for the 3-color Ashkin-Teller model with $\epsilon = 2\sqrt{2}$. The data have been obtained using Algo. 1 with 16 states per site.

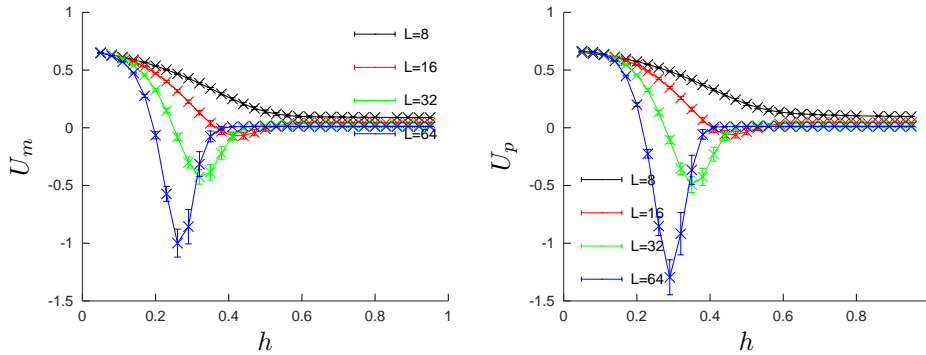


Figure 99. Average Binder cumulant of magnetization (left) and polarization (right) for the 3-color Ashkin-Teller model with $\epsilon = 4$. The data have been obtained using Algo. 1 with 16 states per site.

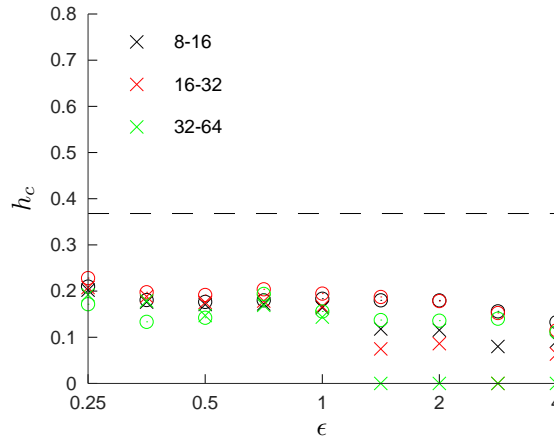


Figure 100. Phase diagram of the 3-color Ashkin-Teller model obtained from the crossings of the Binder cumulants U_m (crosses) and U_p (circles). The colors are associated to the pair of lattice sizes (see the legend) used to find the crossing of the cumulants. The data have been obtained using Algo. 1 with 16 states per site.

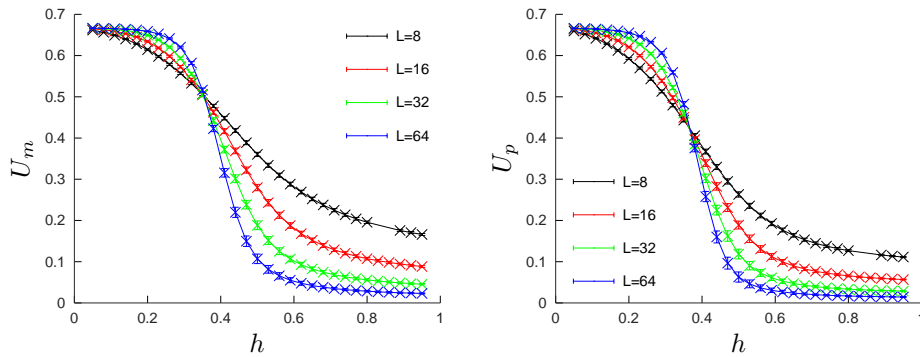


Figure 101. Average Binder cumulant of magnetization (left) and polarization (right) for the 3-color Ashkin-Teller model with $\epsilon = 1/4$. The data have been obtained using Algo. 2 with 16 states per site.

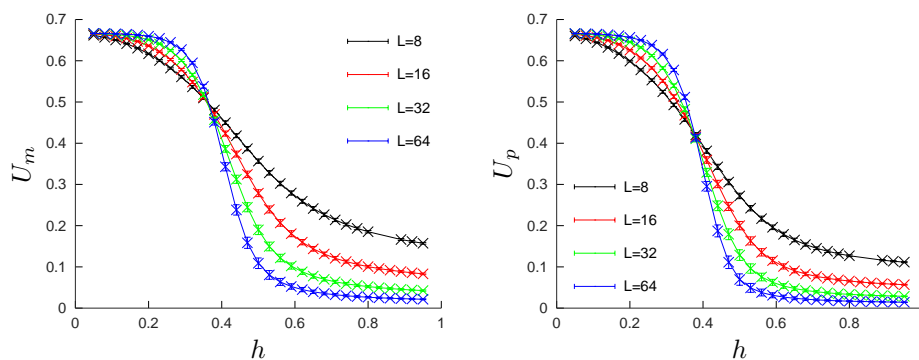


Figure 102. Average Binder cumulant of magnetization (left) and polarization (right) for the 3-color Ashkin-Teller model with $\epsilon = \sqrt{2}/4$. The data have been obtained using Algo. 2 with 16 states per site.

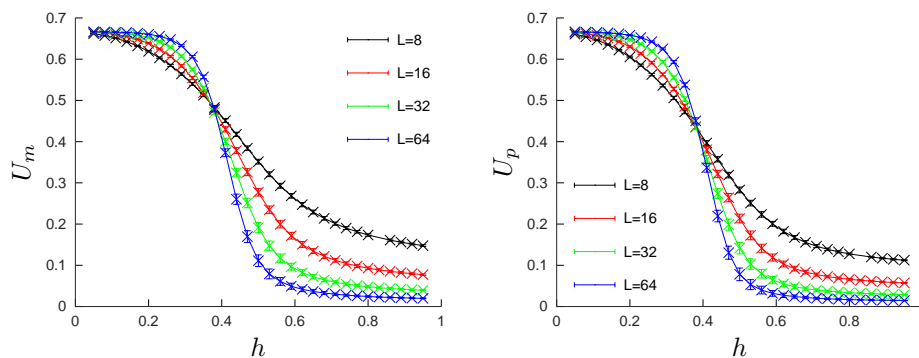


Figure 103. Average Binder cumulant of magnetization (left) and polarization (right) for the 3-color Ashkin-Teller model with $\epsilon = 1/2$. The data have been obtained using Algo. 2 with 16 states per site.

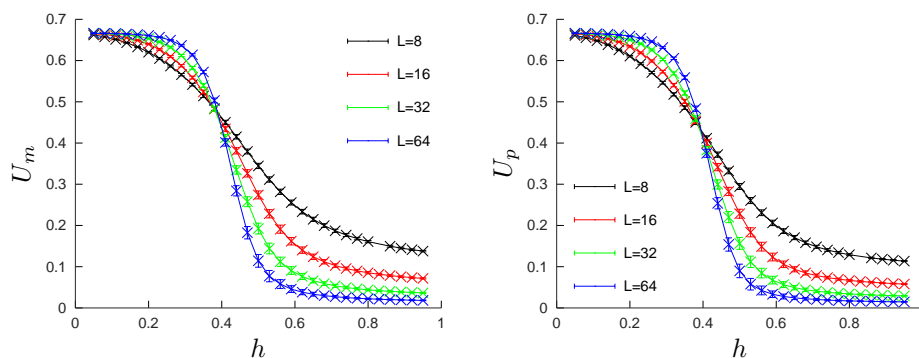


Figure 104. Average Binder cumulant of magnetization (left) and polarization (right) for the 3-color Ashkin-Teller model with $\epsilon = \sqrt{2}/2$. The data have been obtained using Algo. 2 with 16 states per site.

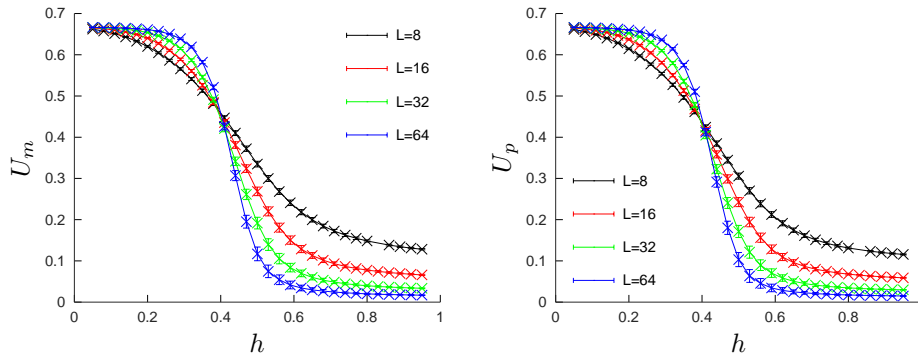


Figure 105. Average Binder cumulant of magnetization (left) and polarization (right) for the 3-color Ashkin-Teller model with $\epsilon = 1$. The data have been obtained using Algo. 2 with 16 states per site.

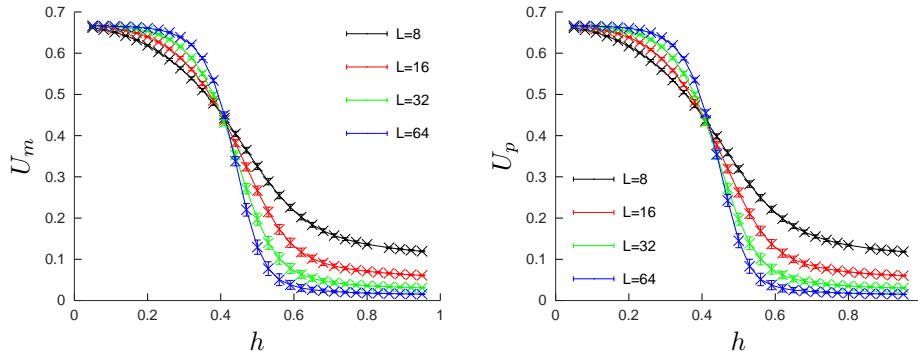


Figure 106. Average Binder cumulant of magnetization (left) and polarization (right) for the 3-color Ashkin-Teller model with $\epsilon = \sqrt{2}$. The data have been obtained using Algo. 2 with 16 states per site.

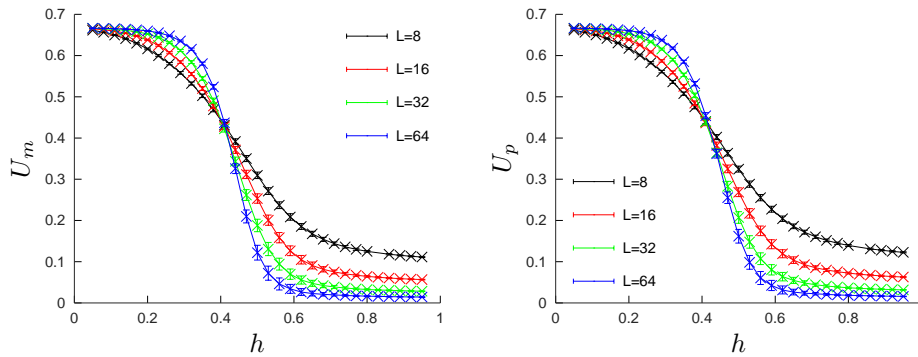


Figure 107. Average Binder cumulant of magnetization (left) and polarization (right) for the 3-color Ashkin-Teller model with $\epsilon = 2$. The data have been obtained using Algo. 2 with 16 states per site.

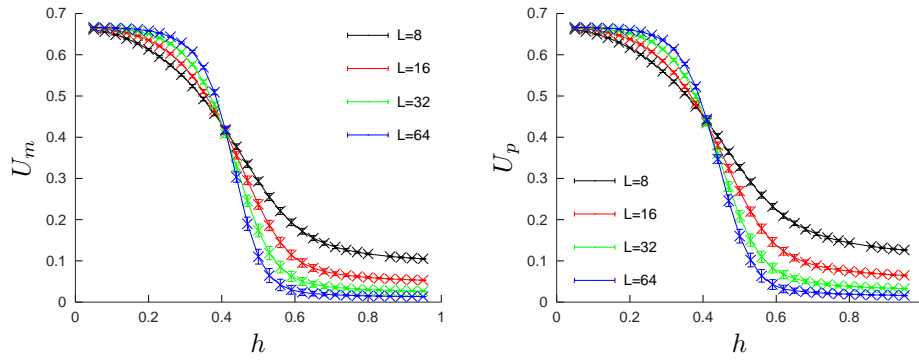


Figure 108. Average Binder cumulant of magnetization (left) and polarization (right) for the 3-color Ashkin-Teller model with $\epsilon = 2\sqrt{2}$. The data have been obtained using Algo. 2 with 16 states per site.

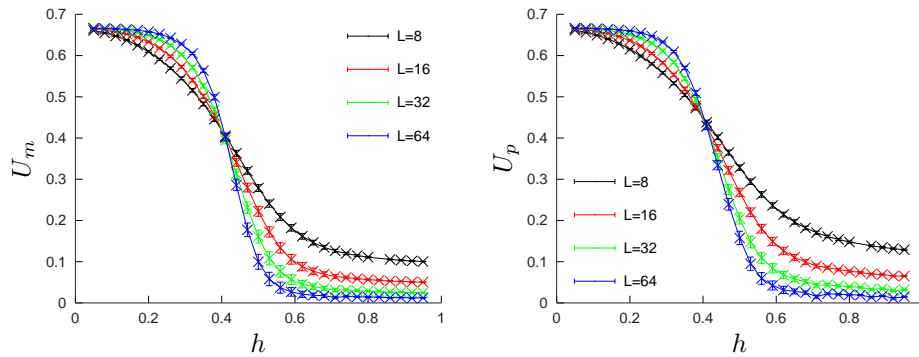


Figure 109. Average Binder cumulant of magnetization (left) and polarization (right) for the 3-color Ashkin-Teller model with $\epsilon = 4$. The data have been obtained using Algo. 2 with 16 states per site.

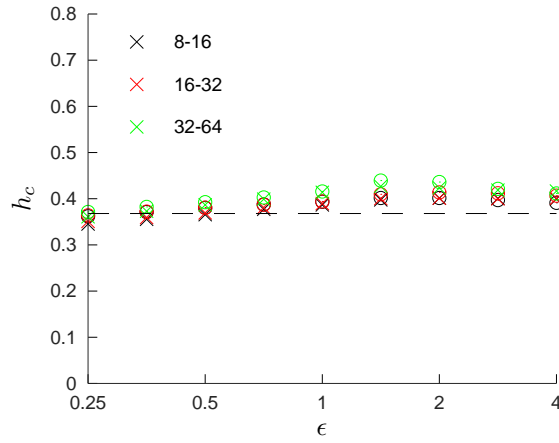


Figure 110. Phase diagram of the 3-color Ashkin-Teller model obtained from the crossings of the Binder cumulants U_m (crosses) and U_p (circles). The colors are associated to the pair of lattice sizes (see the legend) used to find the crossing of the cumulants. The data have been obtained using Algo. 2 with 16 states per site.

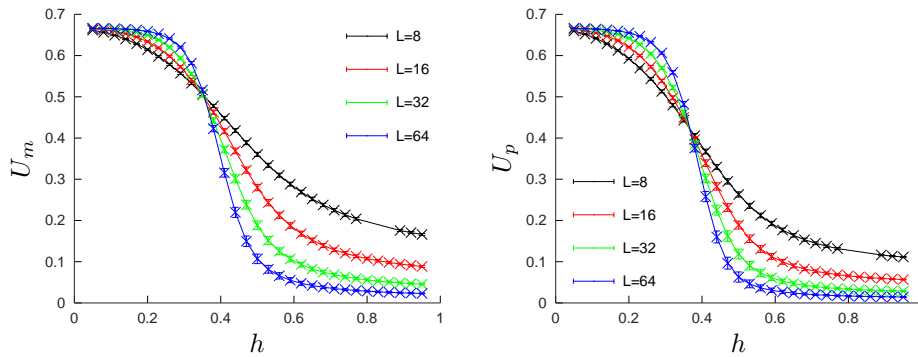


Figure 111. Average Binder cumulant of magnetization (left) and polarization (right) for the 3-color Ashkin-Teller model with $\epsilon = 1/4$. The data have been obtained using Algo. 3 with 16 states per site.

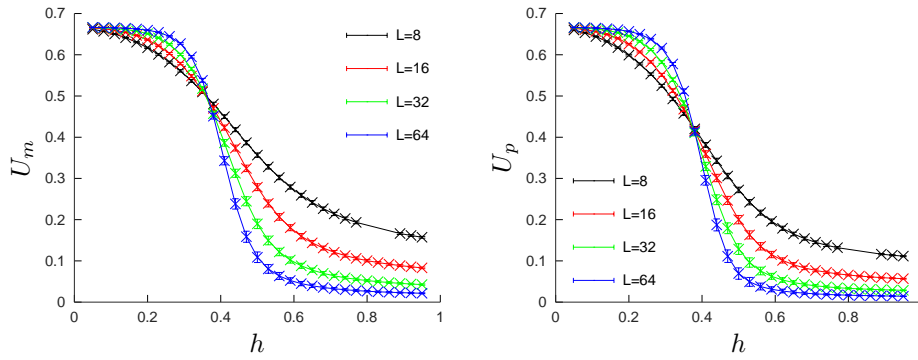


Figure 112. Average Binder cumulant of magnetization (left) and polarization (right) for the 3-color Ashkin-Teller model with $\epsilon = \sqrt{2}/4$. The data have been obtained using Algo. 3 with 16 states per site.

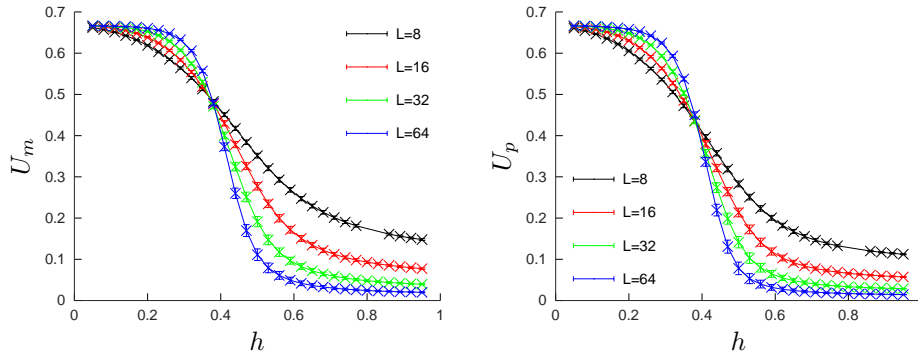


Figure 113. Average Binder cumulant of magnetization (left) and polarization (right) for the 3-color Ashkin-Teller model with $\epsilon = 1/2$. The data have been obtained using Algo. 3 with 16 states per site.

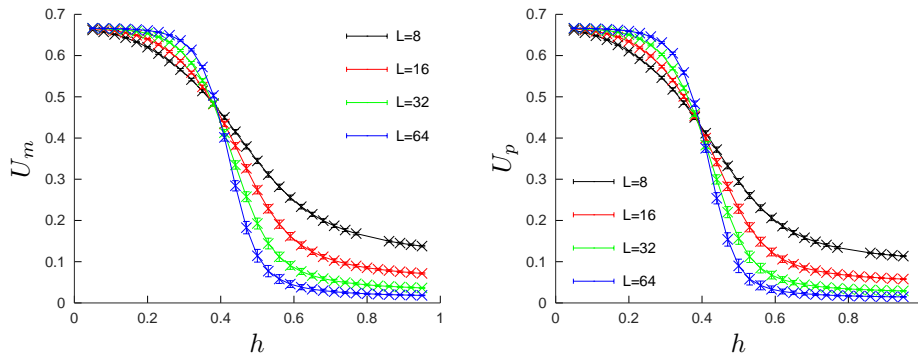


Figure 114. Average Binder cumulant of magnetization (left) and polarization (right) for the 3-color Ashkin-Teller model with $\epsilon = \sqrt{2}/2$. The data have been obtained using Algo. 3 with 16 states per site.

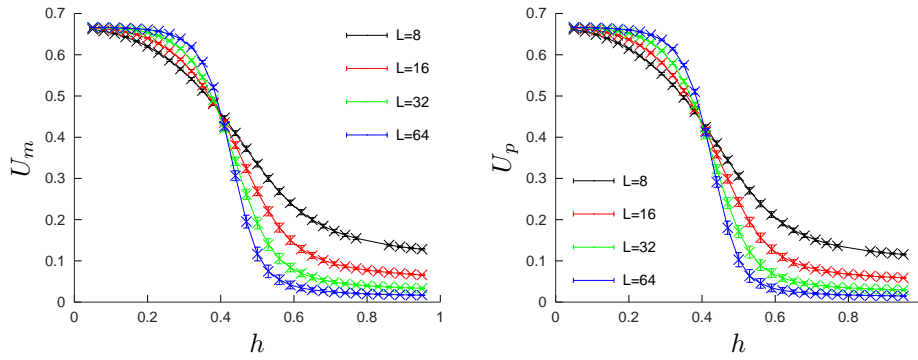


Figure 115. Average Binder cumulant of magnetization (left) and polarization (right) for the 3-color Ashkin-Teller model with $\epsilon = 1$. The data have been obtained using Algo. 3 with 16 states per site.

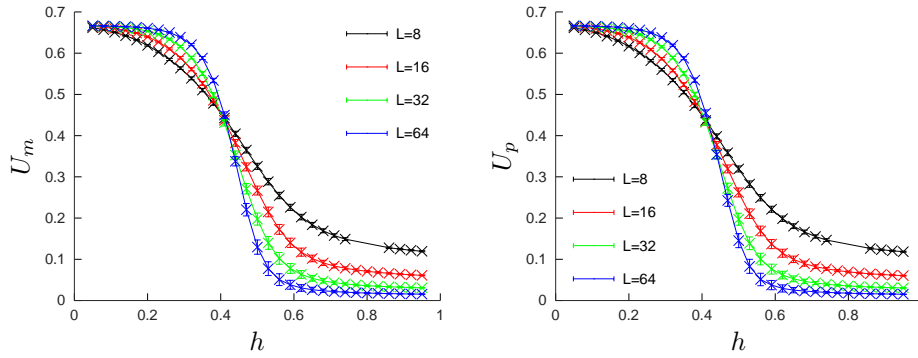


Figure 116. Average Binder cumulant of magnetization (left) and polarization (right) for the 3-color Ashkin-Teller model with $\epsilon = \sqrt{2}$. The data have been obtained using Algo. 3 with 16 states per site.

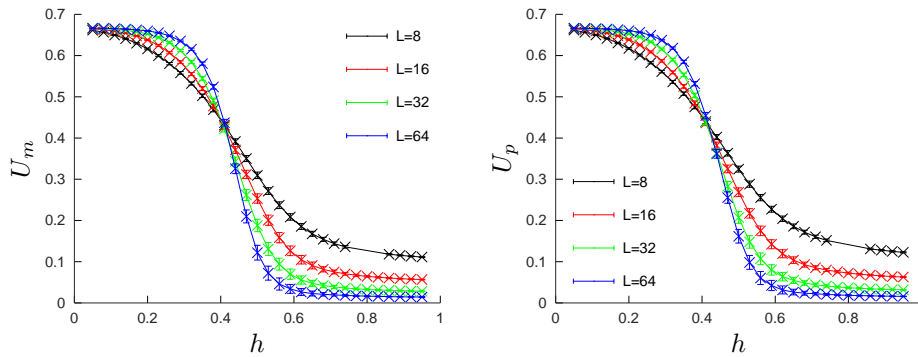


Figure 117. Average Binder cumulant of magnetization (left) and polarization (right) for the 3-color Ashkin-Teller model with $\epsilon = 2$. The data have been obtained using Algo. 3 with 16 states per site.

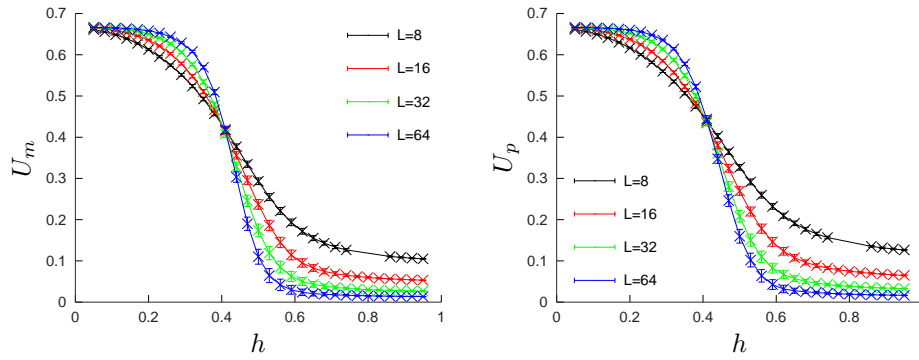


Figure 118. Average Binder cumulant of magnetization (left) and polarization (right) for the 3-color Ashkin-Teller model with $\epsilon = 2\sqrt{2}$. The data have been obtained using Algo. 3 with 16 states per site.

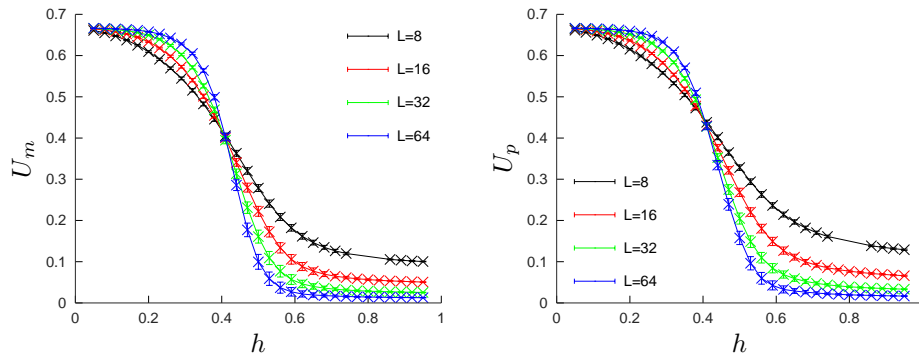


Figure 119. Average Binder cumulant of magnetization (left) and polarization (right) for the 3-color Ashkin-Teller model with $\epsilon = 4$. The data have been obtained using Algo. 3 with 16 states per site.

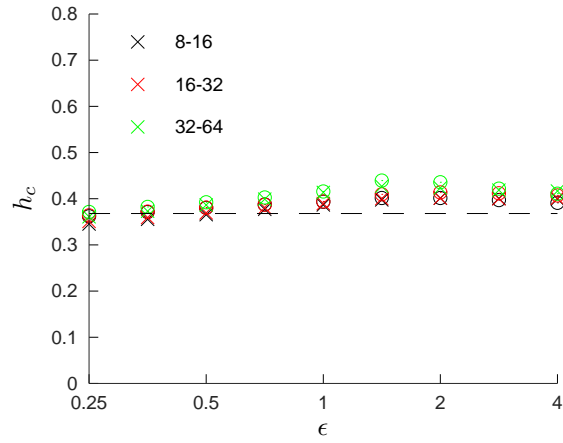


Figure 120. Phase diagram of the 3-color Ashkin-Teller model obtained from the crossings of the Binder cumulants U_m (crosses) and U_p (circles). The colors are associated to the pair of lattice sizes (see the legend) used to find the crossing of the cumulants. The data have been obtained using Algo. 3 with 16 states per site.